

TASI LECTURES ON GRAVITATIONAL WAVES FROM THE EARLY UNIVERSE

ALESSANDRA BUONANNO

groupe de Gravitation et Cosmologie (GReCO)
Institut d'Astrophysique de Paris (CNRS)
98^{bis} Boulevard Arago, 75014 Paris, France
email: buonanno@iap.fr

These lectures discuss how the direct detection of gravitational waves can be used to probe the very early Universe. We review the main cosmological mechanisms which could have produced relic gravitational waves, and compare theoretical predictions with capabilities and time scales of current and upcoming experiments.

1. Overview of gravitational-wave research

In 1916 Einstein realized the propagation effects at finite velocity in the gravitational equations and predicted the existence of wave-like solutions of the linearized vacuum field equations [1]. The work of Bondi [2] in the mid 50s, applied to self-gravitating systems like binaries made of neutron stars and/or black holes, proved that gravitational waves (GWs) carry off energy from those systems, as the 1974 discovery of the binary pulsar PSR 1913+16 by Hulse and Taylor [3] confirmed indisputably. This discovery is an *indirect* observation of GWs. In fact, the speed up of the two-body orbital period can be explained as due to GW emission.

The experimental search for *direct* observation of gravitational waves begun only in the 60s with the pioneering work of Joseph Weber, and for almost three decades it has been pursued solely using meter-scale resonant-bar detectors. These detectors are cylindrical-shape bars whose mechanical oscillations can be driven by GWs. Five cryogenic resonant-bar detectors are in operation since 1990: ALLEGRO, AURIGA, EXPLORER, NAUTILUS and NIOBE [4]. They are narrow-band detectors sensitive to GW frequency \sim kHz. During the last years a world-wide network of kilometer-scale ground-based laser-interferometer detectors has been built and has begun operation in Japan (TAMA 300), in the United States (LIGOs) and Europe (GEO 600 and VIRGO) [5, 6]. The frequency band is $\sim 1-10^3$ Hz.

Meantime the first detectors begin the search, development of the next generation kilometer-scale interferometers is already underway [7, 8, 9, 10]. A laser-interferometer space antenna (LISA) [11, 6] is also planned by the European Space Agency (ESA) and NASA, though not yet fully funded, and could fly in ~ 2011 . It consists of three drag-free spacecrafts in a triangle configuration. The spacecraft tracks the distance to each other (~ 5 million kms) using laser beams, searching GWs in the frequency range $\sim 10^{-4}$ – 10^{-1} Hz. Thanks to the theoretical and experimental progress made by the GW community during the last forty years, the direct detection of GWs is not far ahead of us and, hopefully, it will mark the next decade.

The most promising sources for both ground- and space-based detectors are astrophysical sources at relatively low red-shift [12], like binaries made of black holes (BHs) and/or neutron stars (NSs), white-dwarf (WD) binaries, supermassive black holes, low-mass X-ray binaries, supernovae and pulsars. The large scale interferometers were indeed conceived and designed to detect GWs from those sources. These lectures will focus on cosmological sources at much higher red-shift $z \gg 1$. We shall discuss if and how the detection of GWs can be used to investigate physical processes occurred around Universe's birth. Various excellent lectures and reviews were written on this subject like, e.g., the ones by Allen [13] and Maggiore [14] [see also Sections 2.9 and 3.6 by Cutler and Thorne [12]].

It is not possible to cover in two lectures all the literature on the subject, so we have to make a selection. In the first lecture, after briefly reviewing the key ideas underlying GW detectors [see Section 2], we discuss general features of relic GW spectra, their typical intensity and range of frequencies and phenomenological bounds [see Section 3]. The bulk of the lecture will be the analysis of the phenomenon of amplification of quantum-vacuum fluctuations, and the evaluation of stochastic GW backgrounds in standard, quintessential and superstring-motivated inflationary scenarios [see Section 4]. The second lecture will review, in Section 5, other physical mechanisms which could produce GWs, like first-order phase transitions, turbulence, preheating, etc., and cosmic strings [see Section 6]. Then, in Section 7 we discuss which differences in the relic GW spectrum we could expect from brane-world scenarios and, finally, in Section 8 we comment on the possibility of extracting the red-shift–luminosity curve and cosmological parameters by detecting GWs from binary systems. Section 9 summarizes the conclusions.

2. Key ideas underlying GW detectors

The simplest GW detector we can imagine is a body of mass m at a distance L from a fiducial laboratory point, connected to it by a spring of resonant frequency ω_0 and quality factor Q . Einstein equation of geodesic deviation predicts that the infinitesimal displacement ΔL of the mass along the line of separation from its equilibrium position satisfies the equation [15] (valid for GW wavelengths $\gg L$ and in local Lorentz frame of the observer at the fiducial laboratory point)

$$\ddot{\Delta L}(t) + 2\frac{\omega_0}{Q}\dot{\Delta L}(t) + \omega_0^2\Delta L(t) = \frac{L}{2}\left[F_+\ddot{h}_+(t) + F_\times\ddot{h}_\times(t)\right], \quad (1)$$

where $F_{+,\times}$ are coefficients of order unity which depend on the direction of the source and the GW polarization angle; $h_{+,\times}$ are the two independent polarizations of the GW.

Laser-interferometer GW detectors, such as GEO, LIGO, VIRGO and TAMA, are composed of two perpendicular kilometer-scale arm cavities with two test-mass mirrors hung by wires at the end of each cavity. The tiny displacements ΔL of the mirrors induced by a passing-by GW are monitored with very high accuracy by measuring the relative optical phase between the light paths in each interferometer arm. The mirrors are pendula with quality factor Q quite high and resonant frequency ω_0 much lower (~ 1 Hz) than the typical GW frequency (~ 100 Hz). In this case Eq. (1), written in Fourier domain, reduces to $\Delta L/L \sim h$. The typical amplitude, at 100 Hz, of GWs emitted by binary systems in the VIRGO cluster of galaxies (15 Mpc distant), which is the largest distance the first-generation of ground-based interferometers can probe, is $\sim 10^{-21}$. This means $\Delta L \sim 10^{-18}$ m, a very tiny number! It seems rather discouraging, especially if we think to monitor the test-mass motion with light of wavelength nearly 10^{12} times larger. It took a long time, theoretically and experimentally to develop sophisticated technology to achieve measurements of such tiny displacements.

The electromagnetic signal coming out the interferometer will contain the GW signal but also noise – for example thermal noise in the suspension system and in the mirror itself, can shake the mirror mimicking the effect of a GW. The root-mean-square of the noise is generally expressed in terms of the noise power per unit frequency S_n by the relation $h_{\text{rms}} \sim \sqrt{S_n(f)\Delta f} \sim \Delta L/L$, ΔL being the mirror displacement induced by noise and Δf the frequency bandwidth.

3. Production of relic gravitational waves: general features

3.1. Gravitational-wave spectrum

Since in the following we will focus mainly on the primordial stochastic background of GWs, in this section we relate its energy density to the *spectral density* S_h , which is the quantity of direct interest when we want to compare theoretical predictions to experimental sensitivities. [Henceforth, we pose $\hbar = 1 = c$.]

The intensity of a stochastic background of GWs at (present) frequency f is generally expressed in terms of

$$\Omega_{\text{GW}}(f) = \frac{1}{\rho_c} \frac{d\rho_{\text{GW}}}{d\log f}, \quad (2)$$

where $\rho_c = 3H_0^2/(8\pi G_{\text{N}})$ and ρ_{GW} is the energy density of the GW stochastic background.^a In the transverse-traceless (TT) gauge, denoting with $\hat{\Omega}$ the direction of propagation of the GW, with \hat{m}, \hat{n} the unit vectors forming with $\hat{\Omega}$ an orthonormal basis, and with $\epsilon_{ij}^+ = \hat{m}_i \hat{m}_j - \hat{n}_i \hat{n}_j$, $\epsilon_{ij}^\times = \hat{m}_i \hat{n}_j + \hat{n}_i \hat{m}_j$ the polarization tensors, $i, j = 1, 2, 3$ [$\epsilon_{ij}^{\text{P}}(\Omega) e^{\text{Qij}}(\Omega) = 2\delta^{\text{PQ}}$], a stochastic, isotropic GW can be written as

$$h_{ij}(t) = \sum_{\text{P}=\text{+},\times} \int_{-\infty}^{+\infty} df \int d\hat{\Omega} h_{\text{P}}(f, \hat{\Omega}) e^{-2\pi i f t} \epsilon_{ij}^{\text{P}}(\hat{\Omega}), \quad (3)$$

where $d\hat{\Omega} = d\phi d\cos\theta$, $h_{\text{P}}(f, \hat{\Omega}) = h_{\text{P}}^*(-f, \hat{\Omega})$, and in writing Eq. (3) we have assumed, in full generality, that the wave is located at $\vec{x} = 0$. If the stochastic background is also stationary and unpolarized, averaging the Fourier components over an ensemble gives [14]

$$\langle h_{\text{P}}^*(f, \hat{\Omega}) h_{\text{Q}}(f', \hat{\Omega}') \rangle = \delta(f - f') \delta^2(\hat{\Omega}, \hat{\Omega}') \frac{1}{4\pi} \delta_{\text{PQ}} \frac{1}{2} S_h(f), \quad (4)$$

with $\delta^2(\hat{\Omega}, \hat{\Omega}') = \delta(\cos\theta - \cos\theta') \delta(\phi - \phi')$. The above equation defines the (one-sided) *spectral density* S_h [$S_h(f) = S_h(-f)$], which has the dimensions of Hz^{-1} . The energy density of GWs is given by the 00 component of the energy-momentum tensor averaged over several wavelengths [see e.g., Ref. [15]]

$$\rho_{\text{GW}} = \int_0^\infty d\log f \frac{d\rho_{\text{GW}}}{d\log f} = \frac{1}{32\pi G_{\text{N}}} \overline{h_{ij} \dot{h}^{ij}}. \quad (5)$$

^aThe value of H_0 is generally written as $H_0 = h_0 \times 100 \text{ km/sec/Mpc}$ where h_0 parameterizes the existing experimental uncertainty. Henceforth, all primordial spectrum will be expressed in terms of $h_0^2 \Omega_{\text{GW}}$.

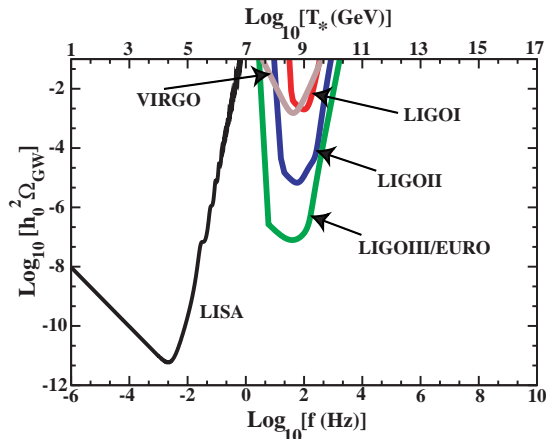


Figure 1. Sensitivities, expressed in terms of Ω_{GW} , versus frequency of LISA and ground-based detectors of first, second and third generation. On the top axis, the estimated temperature of the Universe when GWs are produced by causal mechanisms during RD era [see Eq. (10)].

Inserting in the above equation Eq. (3) and using the property that for a stochastic background the spatial average can be traded with the ensemble average defined by Eq. (4), a straightforward calculation leads to:

$$\Omega_{\text{GW}}(f) = \frac{4\pi^2}{3H_0^2} f^3 S_h(f) \simeq 1.25 \times 10^{36} \frac{1}{h_0^2} \left(\frac{f}{\text{Hz}} \right)^2 f S_h(f). \quad (6)$$

Note that if $\Omega_{\text{GW}} \sim \mathcal{C} f^\alpha$ with $0 \leq \alpha < 3$, due to the factor f^3 appearing in the RHS of Eq. (6), a GW detector operating at lower frequency needs lower sensitivity than a GW detector operating at higher frequency. This explains why space-based detectors like LISA can have better performances than ground-based detectors, although the expected sensitivity of LISA is worse than LIGO and VIRGO.

In Fig. 1 we plot the sensitivities for ground-based detectors of first [5], second (~ 2008) [7, 8] and third (> 2011) [9, 10] generation. More specifically, for the second generation we use the Advanced LIGO configuration or LIGOII [7, 8], for which considerable research and development (R&D) have been gained during the last years, and for the third generation we use, as an example, the speed-meter configuration [9, 10]. The R&D for third generation of interferometers as LIGOIII/EURO started only more recently.

A stochastic background is a random process which is intrinsically indistinguishable from the detector noise. As we shall see in the following, the GW signal is expected to be far too low to exceed the noise level in any existing or planned single detector on the earth. Moreover, the instrumental noise level will not be known sufficiently well a priori to search for excess noise in each instrument. Therefore, the optimal strategy which has been proposed [16] is to perform a correlation between two or more detectors, possibly widely separated to minimize common noise sources. By correlating two detectors the increase in sensitivity h_{rms} is $\sim (\Delta f T)^{1/4}$ where Δf is the bandwidth and T the total observation time. Henceforth, we shall show the sensitivities obtained correlating two ground-based detectors. Assuming a constant GW spectrum, and correlating for fourth months, we obtain at 90% confident level for two LIGO I: $h_0^2 \Omega_{\text{GW}} \simeq 3.5 \times 10^{-6}$, for two LIGO II: $h_0^2 \Omega_{\text{GW}} \simeq 5.1 \times 10^{-9}$ and for two LIGO III: $h_0^2 \Omega_{\text{GW}} \simeq 3.7 \times 10^{-11}$.

In the case of LISA, since only one space-based detector is currently planned, the method of correlating two detectors cannot be used. [In Ref. [17] optimal orbital alignments for correlating a pair of future LISA-kind detectors have been investigated.] Armstrong, Estabrook and Tinto [18] realized that by combining the signals from the three spacecrafts which compose LISA, it is possible to measure the instrumental noise power. Then, any excess noise above this power will be due to GWs. However, besides the primordial stochastic GW background, there are various astrophysically generated stochastic GW background due to binaries present in our galaxy or outside it. These stochastic backgrounds are produced when the incoherent superposition of gravitational radiation emitted by a large number of astrophysical sources cannot be resolved individually. A possible, although rather challenging way of discriminating between the primordial and astrophysically generated backgrounds was suggested by Ungarelli and Vecchio [19]. As LISA rotates along its orbit, its sensitivity to different directions changes, so LISA could measure the isotropy of the stochastic background and use it to separate the primordial stochastic background, which is isotropic, from the galactic stochastic background, which is anisotropic, being concentrated mostly in the galactic plane (rather than in the halo). In Fig. 1 we plot the planned LISA sensitivity [40].

3.2. *When gravitons decoupled: thermal spectrum?*

It is well known that particles which decoupled from primordial plasma at time t_{dec} , when the Universe had temperature T_{dec} , carry information on

the state of the Universe at T_{dec} . The weaker the interaction, the higher the energy scale when they drop out of thermal equilibrium. To estimate T_{dec} for gravitons, we proceed as follows [20, 21]. We assume that gravitons are in thermal equilibrium in the primordial plasma through point-like four-body interactions involving two gravitons. We denote with $\Gamma = n\sigma|v|$ the interaction rate per particle, n being the number density of particles in equilibrium, σ the scattering cross section, and v the relative velocity. From dimensional considerations we expect $\sigma \sim G_{\text{N}}^2 E^2 \sim G_{\text{N}}^2 T^2$, where G_{N} is the Newton constant and E^2 is the average energy squared. For relativistic particles in equilibrium at temperature T , $n \sim T^3$. We also assume $v \sim 1$. The interaction rate is then $\Gamma \sim G_{\text{N}}^2 T^5$. Assuming the Universe evolves adiabatically, we have $g_{\text{S}} T^3 a^3 = \text{const.}$, where g_{S} is the number of effectively massless degrees of freedom [see Eq. (3.73) of Ref. [21]]. Since for relativistic particles $\rho \sim T^4$, we have $\dot{T}/T \propto H \propto T^2/M_{\text{Pl}}$, thus the condition to maintain thermal equilibrium is $\Gamma \gtrsim H$, i.e. the interaction time-scale must exceed the local Hubble time. This gives:

$$\left(\frac{\Gamma}{H}\right)_{\text{g}} \simeq \left(\frac{T}{M_{\text{Pl}}}\right)^3. \quad (7)$$

So, as it could have been anticipated from dimensional considerations, gravitons decoupled at $T_{\text{dec}} \sim M_{\text{Pl}}$. Let us derive at which temperature it corresponds today. The temperature of the Universe, i.e. of the particles in thermal equilibrium, scales as $T \propto g_{\text{S}}^{-1/3} a^{-1}$, while the temperature associated to particles which have decoupled from the thermal bath drops as $T \propto a^{-1}$. Applying these considerations to the thermal bath of gravitons, and using the fact that at $T \gtrsim 300$ GeV the Standard Model (SM) of particle physics predicts $g_{\text{S}} \simeq 106.75$, while at present time, assuming three neutrino species, $g_{\text{S}} \simeq 3.91$, it is easily derived that the graviton temperature today is at most [21] $T_{\text{g}} = (3.91/106.75)^{1/3} 2.75 \text{ K} \simeq 0.9 \text{ K}$ [at most because the effective number of massless degrees of freedom could be higher than 106.75 at Planckian energies.]. Thus, the thermal spectrum of gravitons ranges in the GHz and is given by [13]

$$\Omega_g(f) = \frac{8\pi h}{c^3} \left(\frac{f}{f_g}\right)^4 \frac{1}{\rho_c} \frac{f_g^4}{e^{f/f_g} - 1} \simeq 2.9 \times 10^{-8} h_0^{-2} \left(\frac{f}{f_g}\right)^4 \frac{e - 1}{e^{f/f_g} - 1}, \quad (8)$$

with $f_g = kT_{\text{g}}/h \simeq 1.9 \times 10^{10} \text{ Hz}$. [Note that for CMBR we have $T_{\gamma} \simeq 2.73 \text{ K}$ and $f_{\gamma} = 5.7 \times 10^{10} \text{ Hz}$.] However, since gravitons interact very weakly with matter and radiation, the time required to reach thermal equilibrium could be longer than the Hubble time. So, it is quite unlikely that this

radiation ever existed. Moreover, if the Universe underwent a period of inflation after the Planck era, the background should have been strongly diluted. More importantly, the theory of gravity at the Planck energy could differ significantly from Einstein theory; if so, the above analysis should be modified, accordingly.

3.3. *Gravitational waves produced by casual mechanisms: typical frequencies*

Two features determine the typical frequency of GWs of cosmological origin produced by some casual mechanism [14]: (i) the dynamics, which is model dependent, and (ii) the kinematics, that is the red-shift from the production era.

Let us assume that a graviton is produced with frequency f_* at time t_* during RD or MD era. We want to evaluate its frequency today $f = f_* a_*/a_0$. Assuming that the Universe evolved adiabatically, that is $g_S(T_*) T_*^3 a_*^3 = g_S(T_0) T_0^3 a_0^3$, and using $T_0 = 2.73K$ and $g_S = 3.91$ we get

$$f \simeq 10^{-13} f_* \left(\frac{100}{g_{S*}} \right)^{1/3} \left(\frac{1\text{GeV}}{T_*} \right). \quad (9)$$

Since the size of the Hubble radius is the length scale beyond which causal microphysics cannot operate, from causality considerations we expect the characteristic wavelength of gravitons produced at time t_* is either $\sim H_*^{-1}$ or smaller. So, we pose [14] $\lambda_* = \epsilon H_*^{-1}$ with $\epsilon \lesssim 1$. If the GW signal is produced during RD era $H_*^2 = 8\pi G_N \rho_{\text{rad}}/3 = 8\pi^3 g_* T_*^4 / (90 M_{\text{Pl}}^2)$ and

$$f \simeq 10^{-7} \frac{1}{\epsilon} \left(\frac{T_*}{1\text{GeV}} \right) \left(\frac{g_*}{100} \right)^{1/6} \text{Hz}. \quad (10)$$

On the top axis of Fig. 1 we show the production temperature T_* as obtained from Eq. (10) by expressing T_* in terms of the frequency f . For the kind of mechanism analysed in this section, LISA could probe physics at TeV scale, ground-based interferometers in the range $\sim 10^8$ – 10^{10} GeV, while GUT and Planck scales could be probed in GHz region, where however no GW detectors have been planned so far, but electromagnetic (EM) microwave cavities have been proposed [22].

3.4. *Phenomenological bounds*

3.4.1. *Big-bang nucleosynthesis bound*

The theory of Big-bang nucleosynthesis (BBN) [23] predicts rather successfully the primordial abundances of light elements like deuterium, ^3He , ^4He

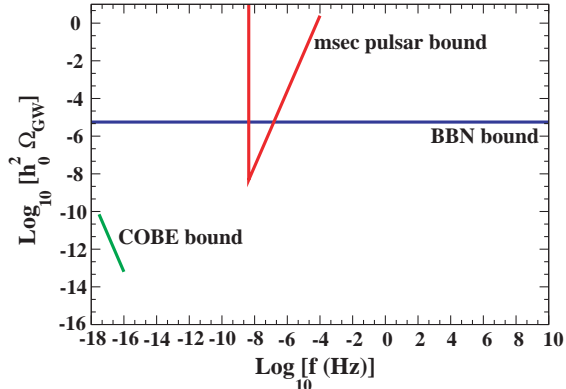


Figure 2. Summary of phenomenological bounds on energy density of relic GWs.

and ${}^7\text{Li}$. If at nucleosynthesis time ($T \simeq \text{MeV}$), the contribution of the primordial GWs to the total energy density is too large, then the expansion rate of the Universe H , and the freeze-out temperature which determines the relative abundance of neutrons and protons, will be too high. Thus, neutrons will be more available and ${}^4\text{He}$ will be overproduced, spoiling BBN predictions. Detailed calculations provides the following bound on the energy density in GWs integrated over frequency,

$$\int_{f=0}^{f=+\infty} d \log f h_0^2 \Omega_{\text{GW}}(f) \leq 5.6 \times 10^{-6} (N_\nu - 3), \quad (11)$$

where N_ν is the effective number of neutrino species. The bound (11) holds only for GWs that were already produced at time of nucleosynthesis. Since the integral cannot exceed the bound, also its positive definite integrand cannot do it, unless $\Omega_{\text{GW}} \ll 10^{-6}$ for most of the frequency range and has a very narrow peak on the order of $\sim 10^{-5}$ at some frequency. This possibility is however not very plausible. Thus, Eq. (11) gives for $\Delta f \sim f$ and $N_\nu < 4$ [24] the value $h_0^2 \Omega_{\text{GW}} \leq 5.6 \times 10^{-6}$, which is plotted in Fig. 2.

3.4.2. COBE bound

The COBE bound comes from the measurement of temperature fluctuations in the Cosmic Microwave Background Radiation (CMBR). Indeed, a background of GWs at very low frequencies can produce, if sufficiently

strong, a stochastic red-shift of the CMBR frequencies, through the well known Sachs-Wolfe effect. Indicating by δT the fluctuation induced in the CMBR temperature, we have

$$\Omega_{\text{GW}}(f) \leq \left(\frac{H_0}{f}\right)^2 \left(\frac{\delta T}{T}\right)^2 \quad 3 \times 10^{-18} \text{ Hz} < f < 10^{-16} \text{ Hz}, \quad (12)$$

where the range of frequencies is determined by the condition the GWs are inside the Hubble radius today ($f > H_0 \sim 3 \times 10^{-18} \text{ Hz}$) and they were outside the Hubble radius at the last scattering surface (LSS) ($f < \sqrt{z_{\text{LSS}}} H_0 \sim 10^{-16} \text{ Hz}$ with $z_{\text{LSS}} \sim 10^3$). The value of $\delta T/T$ induced by GWs on CMBR cannot exceed the observed value $\delta T/T \sim 5 \times 10^{-6}$. Detailed analyses give [25, 13]:

$$h_0^2 \Omega_{\text{GW}}(f) < 7 \times 10^{-11} \left(\frac{H_0}{f}\right)^2 \quad 3 \times 10^{-18} \text{ Hz} < f < 10^{-16} \text{ Hz}. \quad (13)$$

GWs can saturate this bound if the contribution from scalar perturbations is subdominant, and this depends on the specific inflationary model. The COBE bound (13) is shown in Fig. 2.

3.4.3. msec pulsar bound

The very accurate timing of msec pulsars constraints Ω_{GW} . In fact, if a GW passes between us and the pulsar the time of arrival of the pulse is (doppler) shifted. Many years of observations lead to the bound [26, 14]

$$h_0^2 \Omega_{\text{GW}}(f) \leq 4.8 \times 10^{-9} \left(\frac{f}{f_*}\right)^2 \quad f > f_* \equiv 4.4 \times 10^{-9} \text{ Hz}, \quad (14)$$

where f_* is derived from the total observation time of ~ 8 years [see Fig. 2].

4. Amplification of quantum vacuum fluctuations

The amplification of quantum vacuum fluctuations is a very general mechanism characterizing quantum field theory in curved space time, first discussed in cosmology by Grishchuk [27] and Starobinsky [28]. Let us first give a formal description of it.

We assume that the background field dynamics is described by the action:

$$S = \frac{1}{16\pi G_{\text{N}}} \int d^4x \sqrt{|g|} \mathcal{R} + S_m, \quad (15)$$

where \mathcal{R} is the Ricci scalar, S_m refers to possible matter sources with $\sqrt{|g|}T_{\mu\nu} = 2\delta S_m/\delta g^{\mu\nu}$, $T_{\mu\nu}$ being the energy-momentum tensor. We restrict ourselves to an isotropic and spatially homogeneous Friedmann-Lemaître-Robertson-Walker (FLRW) unperturbed metric, with scale factor a and $ds^2 = g_{\mu\nu} dx^\mu dx^\nu = -dt^2 + a^2(t) d\vec{x}^2$. The free linearized wave equation for the TT metric perturbations $\delta g_{\mu\nu} = h_{\mu\nu}$ ($h_{\mu 0} = 0, \nabla_\mu h^\mu_\nu = 0, h^\mu_\mu = 0$) can be obtained by perturbing Einstein equations and keeping all the sources fixed, $\delta T_\mu{}^\nu = 0$. A straightforward calculation gives:

$$\square h_i^j(t, \vec{x}) = \frac{1}{\sqrt{|g|}} \partial_\mu (\sqrt{|g|} g^{\mu\nu} \partial_\nu) h_i^j(t, \vec{x}) = 0. \quad (16)$$

Introducing the conformal time η , with $d\eta = dt/a(t)$ and writing

$$h_i^j(\eta, \vec{x}) = \sqrt{8\pi G_N} \sum_{P=+, \times} \sum_{\vec{k}} h_{\vec{k}}^P(\eta) e^{i\vec{k}\cdot\vec{x}} \epsilon_i^{Pj}(\hat{\Omega}), \quad (17)$$

each polarization mode $h_{\vec{k}}^P(\eta)$ satisfies the equation

$$h_{\vec{k}}''(\eta) + 2\frac{a'}{a} h_{\vec{k}}'(\eta) + k^2 h_{\vec{k}}(\eta) = 0, \quad (18)$$

where we indicate with a prime the derivative with respect to conformal time η .

For simplicity let us consider two cosmological phases I and II, e.g., inflation and RD or MD phase. We denote with $h_{\vec{k}}(\eta)$ and $H_{\vec{k}}(\eta)$ the solution of Eq. (18) when the scale factor of phase I and II is used, respectively. The mode expansion of h_i^j in phase I reads:

$$h_i^j = \sqrt{8\pi G_N} \sum_{\mathbf{P}} \int \frac{d^3k}{\sqrt{2k} (2\pi)^3} \left[b_{\mathbf{P}}^{\mathbf{I}}(\vec{k}) h_{\vec{k}}(\eta) \epsilon_i^{\mathbf{P}j}(\hat{\Omega}) e^{i\vec{k}\cdot\vec{x}} + \text{H.C.} \right], \quad (19)$$

where H.C. stands for hermitian conjugate, $b_{\mathbf{P}}^{\mathbf{I}}(\vec{k})$ is the annihilation operator with respect to the vacuum in phase I, i.e. $b_{\mathbf{P}}(\vec{k})|0\rangle_{\mathbf{I}} = 0$ with $\mathbf{P} = \times, +$ [classically, it can be traded with a random variable.] We refer to \vec{x} and \vec{k} as the comoving coordinate and momentum, related to the physical quantities by $\vec{x}_{\text{phys}} = a(t) \vec{x}$ and $\vec{k}_{\text{phys}} = \vec{k}/a(t)$. The mode expansion of H_i^j in the phase II can be obtained from Eq. (19) with the substitution $h_{\vec{k}} \rightarrow H_{\vec{k}}$, $b_{\mathbf{P}}^{\mathbf{I}}(\vec{k}) \rightarrow b_{\mathbf{P}}^{\mathbf{II}}(\vec{k})$. The annihilation operator of phase II satisfies the equations $b_{\mathbf{P}}^{\mathbf{II}}(\vec{k})|0\rangle_{\mathbf{II}} = 0$ with $\mathbf{P} = \times, +$. The quantities $\{h_{\vec{k}}, h_{\vec{k}}^*\}$ and $\{H_{\vec{k}}, H_{\vec{k}}^*\}$ are complete bases and can be related to each other by the so-called Bogoliubov transformation [29]

$$H_{\vec{k}} = \sum_{\vec{k}'} (\alpha_{\vec{k}\vec{k}'} h_{\vec{k}'} + \beta_{\vec{k}\vec{k}'} h_{\vec{k}'}^*), \quad (20)$$

$$h_{\vec{k}} = \sum_{\vec{k}'} (\alpha_{\vec{k}\vec{k}'}^* H_{\vec{k}'} - \beta_{\vec{k}\vec{k}'} H_{\vec{k}'}^*). \quad (21)$$

Note that the above equations express the positive-frequency components of the operator in phase I in terms of *both* the positive and negative components of the operators in phase II, and viceversa. The coefficients $\alpha_{\vec{k}\vec{k}'}$ and $\beta_{\vec{k}\vec{k}'}$ are called Bogoliubov coefficients and satisfy the equations [29]

$$\sum_{\vec{k}} \left[\alpha_{\vec{k}_1 \vec{k}} \alpha_{\vec{k}_2 \vec{k}}^* - \beta_{\vec{k}_1 \vec{k}} \beta_{\vec{k}_2 \vec{k}}^* \right] = \delta_{\vec{k}_1 \vec{k}_2}, \quad (22)$$

$$\sum_{\vec{k}} \left[\alpha_{\vec{k}_1 \vec{k}} \beta_{\vec{k}_2 \vec{k}} - \beta_{\vec{k}_1 \vec{k}} \alpha_{\vec{k}_2 \vec{k}} \right] = 0. \quad (23)$$

Inserting $H_{\vec{k}}$, given by Eq. (20), in the expression of H_i^j and equating to h_i^j , we find the well-known relation between annihilation and creation operators in the two phases:

$$b^{\text{I}}(\vec{k}) = \sum_{\vec{k}'} \left[\alpha_{\vec{k}'\vec{k}} b^{\text{II}}(\vec{k}') + \beta_{\vec{k}'\vec{k}}^* b^{\text{II}\dagger}(\vec{k}') \right], \quad (24)$$

$$b^{\text{II}}(\vec{k}) = \sum_{\vec{k}'} \left[\alpha_{\vec{k}\vec{k}'}^* b^{\text{I}}(\vec{k}') - \beta_{\vec{k}\vec{k}'} b^{\text{I}\dagger}(\vec{k}') \right]. \quad (25)$$

Thus, if $\beta_{\vec{k}\vec{k}'} \neq 0$, even starting from the vacuum ${}_{\text{I}}\langle 0|b^{\text{I}\dagger}(\vec{k})b^{\text{I}}(\vec{k})|0\rangle_{\text{I}} = 0$, we end up with a final number of particles given by

$${}_{\text{I}}\langle 0|b^{\text{II}\dagger}(\vec{k})b^{\text{II}}(\vec{k})|0\rangle_{\text{I}} = \sum_{\vec{k}'} |\beta_{\vec{k}\vec{k}'}|^2 \neq 0. \quad (26)$$

This phenomenon is known as *amplification of quantum-vacuum fluctuations* in curved space time. It is due to the inevitable presence of positive and negative components in the basis I when expressed in terms of the basis II [see Eqs. (20)]. The existence of the two complete bases, which are associated to two independent Fock spaces, is a consequence of being the space-time curved.

The physical idea underlying the quantum-vacuum production of particles can be also explained as follows [14]. [Henceforth, we assume an isotropic and spatially homogeneous metric, so we can pose $\alpha_{\vec{k}\vec{k}'} = \alpha_k \delta_{\vec{k}\vec{k}'}$ and $\beta_{\vec{k}\vec{k}'} = \beta_k \delta_{\vec{k}\vec{k}'}$.] Suppose that over a time-scale $\Delta T \sim H^{-1}$ the cosmological phase changes, e.g., from phase I to phase II. If t_* is the time at which the transition occurs and f_* is the physical frequency of the mode at that time, there exist two possible regimes: abrupt transition for which $2\pi f_* H_*^{-1} \ll 1$ and adiabatic transition $2\pi f_* H_*^{-1} \gg 1$. Let us

assume that the quantum state $|q\rangle$ before the transition has number of particles $N_k^I \equiv \langle q|b_k^{I\dagger} b_k^I|q\rangle$. For modes for which the transition is sudden, i.e. $2\pi f_* H_*^{-1} \ll 1$ (for these modes $\lambda \gg H_*^{-1}$, that is their wavelengths are larger than the Hubble radius or in jargon they are said to be *outside the horizon*, the physical state does not have time to change during the transition. However, after the transition, the number of particles should be evaluated from annihilation and creation operators of phase II,

$$N_k^{II} \equiv \langle q|b_k^{II\dagger} b_k^{II}|q\rangle = N_k^I (1 + 2|\beta_k|^2) + |\beta_k|^2. \quad (27)$$

Therefore, if the number of particles when inflation starts is N_k^I , this number is amplified by the factor $1 + 2|\beta_k|^2$ [33, 14]. Moreover, due to the mixing between positive and negative frequencies even the vacuum state of phase I ($N_k^I = 0$) is a multiparticle state when referred to the vacuum state of phase II. On the other hand, for modes for which the transition is adiabatic, i.e. $2\pi f_* H_*^{-1} \gg 1$ (for these modes $\lambda \ll H_*^{-1}$, so their wavelengths are smaller than the Hubble radius or in jargon these modes are said to be *inside the horizon*), the quantum state has the time to follow the evolution of the scale factor. No particle production occurs in this case. In some sense the modes for which the transition is adiabatic, do not feel any effect of being the spacetime curved or changing in time. No mixing between positive and negative frequencies occurs, as it is in flat spacetime. [Practically, the relic GWs spectrum drops off exponentially for frequencies larger than $f_*^{\text{cutoff}} \sim H_*/(2\pi)$, i.e. for modes which never went outside the Hubble radius.]

We want now to give a more intuitive explanation of the phenomenon of amplification of quantum-vacuum fluctuations, which is very close to the original derivation due to Grishchuk [27] and Starobinsky [28]. It is based on a semiclassical approach. By introducing the variable $\psi_k(\eta) = a h_k(\eta)$, h_k being one of the two polarization modes, Eq. (18) can be recast in the form

$$\psi_k'' + [k^2 - U(\eta)] \psi_k = 0, \quad U(\eta) = \frac{a''}{a}, \quad (28)$$

which is the equation of an harmonic oscillator in the time-dependent potential $U(\eta)$. [Note that to get unambiguous results, the change of variables $\psi(k) \rightarrow h(k)$ can be used only if the scale factor and its first derivative are continuous at the transition between phase I and II [30].] For simplicity, let us consider a de Sitter inflationary era, i.e. $a = -1/(\eta H_{\text{dS}})$, H_{dS} being the constant Hubble parameter during de Sitter phase.

If $k^2 \ll |U(\eta)|$, since $|U(\eta)| \sim \eta^{-2}$ and $(a H_{\text{dS}}) \sim 1/\eta$, then $k\eta \ll 1$, which means $k/a \ll H_{\text{dS}}$ or $\lambda \gg H_{\text{dS}}^{-1}$, i.e. the mode is outside the Hubble radius (or in jargon under the potential barrier $|U(\eta)|$). In this case the solution of Eq. (28) is

$$\psi_k \sim a \left[A_k + B_k \int \frac{d\eta}{a^2(\eta)} \right] \rightarrow h_k \sim A_k + B_k \int \frac{d\eta}{a^2(\eta)}. \quad (29)$$

Since during de Sitter era the scale factor gets larger and larger, the second term in the RHS of Eq. (29) for h_k becomes more and more negligible, thus the tensorial perturbation h_k remains (almost) constant while outside the Hubble radius. On the other hand, if $k^2 \gg |U(\eta)|$, we have $k\eta \gg 1$ or $\lambda \ll H_{\text{dS}}^{-1}$, which means the mode is inside the Hubble radius (or in jargon over the potential barrier $|U(\eta)|$). The solution of Eq. (28) is a plane wave $\psi_k \sim e^{\pm ik\eta}$. Thus, in this case the tensorial perturbation $h_k \sim e^{\pm ik\eta}/a$ decreases in time while inside the Hubble radius. Therefore, in de Sitter case, the longer the tensorial-perturbation mode remains outside the Hubble radius, the more it gets amplified. When the fluctuations re-enter the Hubble radius, the solution of Eq. (28) is

$$\psi_k \sim \alpha_k e^{-ik\eta} + \beta_k e^{ik\eta}, \quad (30)$$

and contains both positive and negative modes. The coefficient β_k is the Bogoliubov coefficient and it can be determined imposing the continuity of ψ_k and ψ'_k all along the cosmological phases.

Before ending this section we want to express the intensity of the stochastic GW background (2) in terms of the number of gravitons per cell of the phase space, which we indicate by n_f with $f = |\vec{k}|/(2\pi)$. In the case of GWs produced out of vacuum, $n_f = N_f^{\text{II}}$, thus it is the crucial quantity to evaluate. For an isotropic stochastic GW background $\rho_{\text{GW}} = 2 \int d^3k/(2\pi)^3 (k n_k)$, thus

$$\Omega_{\text{GW}}(f) = \frac{1}{\rho_c} 16\pi^2 n_f f^4. \quad (31)$$

From the above expression it is straightforward to deduce that if the planned space- and ground- based GW experiments will detect a stochastic GW background whose spectrum satisfies the BBN phenomenological bound discussed in Section 3.4.1, i.e. $\Omega_{\text{GW}} < 10^{-6}$, the occupation number $n_f \gg 1$. This means the observed stochastic GW background is classical.

4.1. Standard inflation

In this section we shall first derive the GW spectrum in de Sitter inflation, which although is an ideal case (because it does not lead naturally to the transition from inflation to RD era), it has the advantage of providing analytical solutions for the tensorial perturbations. Secondly, we discuss how the GW spectrum is modified in more realistic inflationary scenarios, like slow-roll inflation.

4.1.1. de Sitter inflation

The scale factor during de Sitter era is $a(\eta) = -1/(H_{\text{dS}} \eta)$ with $-\infty < \eta < \eta_*$, while during the RD era we have $a(\eta) = (\eta - 2\eta_*)/(H_{\text{dS}} \eta_*^2)$ with $\eta_* < \eta < \eta_{\text{eq}}$, where η_{eq} is the time at which there is equality between radiation and matter era. [Henceforth, we refer to quantities evaluated at present time with the subscript 0.]

Let us observe that during de Sitter phase any (classical) tensorial perturbation is *de-amplified* and their wavelength gets always stretched. Indeed, for a given comoving wavenumber k , it can be easily found [31] that the de-amplification coefficient is $\mathcal{A}(f) = h(f, \eta_0)/h(f_{\text{in}}, \eta_{\text{in}}) = e^{-\mathcal{N}} (H_{\text{dS}} a_*/(H_0 a_0))$, where $f = k/(2\pi a_0)$, $f_{\text{in}} = k/(2\pi a_{\text{in}})$ and $\mathcal{N}_{\text{in}} \equiv \log(a_*/a_{\text{in}})$ is the number of e-foldings. [To solve the *horizon* problem [32] the minimal amount of e-foldings is $\mathcal{N}_{\text{min}} = \log(H_{\text{dS}} a_*/(H_0 a_0))$.] Thus, the longer the inflationary era, the smaller the coefficient \mathcal{A} . Moreover, the stretching of the wavelength is $\lambda/\lambda_{\text{in}} = e^{\mathcal{N}} (a_0/a_*)$.

In de Sitter case Eq. (18) can be solved exactly and the solutions are rather simple,^b they read:

$$h_k(\eta) = \frac{1}{a} \left(1 - \frac{i}{k\eta} \right) e^{-ik\eta}, \quad -\infty < \eta < \eta_* \quad (32)$$

$$h_k(\eta) = \frac{1}{a} [\alpha_k e^{-ik\eta} + \beta_k e^{ik\eta}], \quad \eta_* < \eta < \eta_{\text{eq}}. \quad (33)$$

[Here, we have assumed that the initial state of the Universe is the Bunch-Davis vacuum [33], so in Eq. (27) we could unambiguously set $N_k^1 = 0$. See Ref. [34] where this assumption is relaxed.] The Bogoliubov coefficients α_k and β_k in Eq. (33) are obtained imposing the continuity of h_k and h'_k across the transition. A straightforward calculation [33] gives $\beta_k = 1/(2k^2 \eta_*^2)$, so the occupation number is $N_k = |\beta_k|^2$. Using the following relations:

^bThese solutions can be obtained easily rewriting Eq. (18) in terms of the function u_k , defined by $h_k = (a u_k)' / a^2$.

$k|\eta_*| = 2\pi f a_0 |\eta_*| = 2\pi f a_0 / (a_* H_{\text{dS}})$ where $a_* = 1/(H_{\text{dS}} |\eta_*|)$, $a_0/a_* = (t_0/t_{\text{eq}})^{2/3} (t_{\text{eq}}/t_*)^{1/2}$, we obtain $k|\eta_*| = f/f_*$ with

$$f_* = \left(\frac{t_*}{t_{\text{eq}}}\right)^{1/2} \frac{H_{\text{dS}}}{2\pi} \frac{1}{1+z_{\text{eq}}} = 10^9 \left(\frac{H_{\text{dS}}}{6 \times 10^{-5} M_{\text{Pl}}}\right)^{1/2} \text{ Hz}, \quad (34)$$

where we used $z_{\text{eq}} \sim 10^4$, $t_{\text{eq}} \sim 10^{10}$ s and $t_* = H_{\text{dS}}/2$. The frequency f_* is the cutoff frequency beyond which the GW spectrum falls down exponentially. By using Eq. (31) with $n_k = 1/(4k^4 \eta_*^4)$, it is straightforward to find that the GW spectrum for fluctuations that re-enter the Hubble radius during the RD era is then

$$h_0^2 \Omega_{\text{GW}}(f) \simeq 4 \times 10^{-14} \left(\frac{H_{\text{dS}}}{6 \times 10^{-5} M_{\text{Pl}}}\right)^2. \quad (35)$$

For fluctuations that re-enter the Hubble radius during the matter era, a similar calculation gives [33]:

$$h_0^2 \Omega_{\text{GW}}(f) \simeq 4 \times 10^{-14} \left(\frac{f_{\text{eq}}}{f}\right)^2 \left(\frac{H_{\text{dS}}}{6 \times 10^{-5} M_{\text{Pl}}}\right)^2, \quad (36)$$

where $f_{\text{eq}} = H_{\text{eq}}/(2\pi)/(1+z_{\text{eq}}) \sim 10^{-16}$ Hz. The COBE bound discussed in Section 3.4.2 imposes that the Hubble parameter during the de Sitter phase should be $< 6 \times 10^{-5} M_{\text{Pl}}$ [35].

4.1.2. *Slow-roll inflation*

As a more realistic example we now discuss slow-roll inflation [32]. In this scenario a scalar field (the inflaton field) drives a period of accelerated expansion by rolling toward the minimum of its potential $V(\phi)$. [Inflation can occur if the slow-roll conditions are satisfied [32]: $\dot{\phi}^2 \ll V(\phi)$ and $|\ddot{\phi}| \ll |3H\dot{\phi}|, |V'| \equiv |dV/d\phi|$.] Differently from de Sitter inflation, in this case the Hubble parameter is not exactly constant during the inflation era, it slowly decreases in time, and as a consequence, the GW spectrum for fluctuations that go out of the Hubble radius during the inflation era and re-enter during RD era, is not flat but acquires a tilt: $h_0^2 \Omega_{\text{GW}}(f) \sim \bar{V} f^{n_T}$,^c where we denote by \bar{V} the value of the inflaton potential at the time the present Hubble scale crossed the Hubble radius during inflation. The spectral slope

^cWhereas in de Sitter inflation the amplitude of the GW spectrum depends on the square of the (constant) Hubble parameter H_{dS} [see Eqs. (35), (36)], in potential-driven inflation, it depends on \bar{V} . Indeed, by applying the slow-roll conditions to the FLRW equations it can be easily seen that $H^2 \simeq 8\pi G_{\text{N}} V/3$.

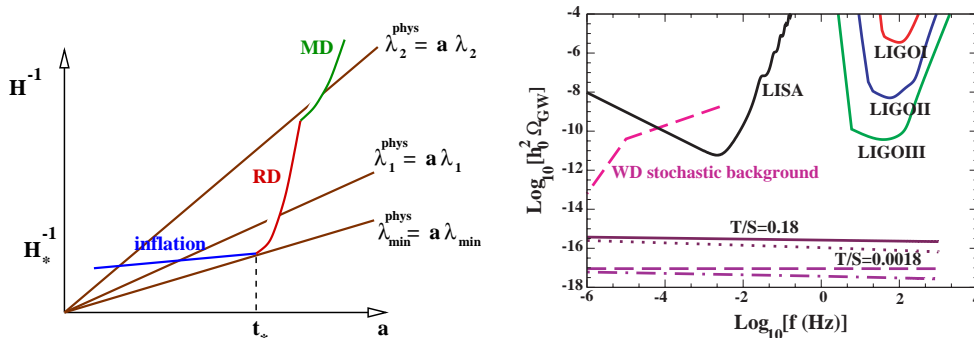


Figure 3. In the left panel we sketch the evolution of the expansion rate of the Universe H and of some physical wavelengths during a period of standard inflation, followed by RD and MD eras. In the right panel we plot the stochastic GW background for slow-roll inflation obtained in Ref. [36] for $T/S = 0.18$ and $dn_T/d\log k = 0$ (continuous line), $T/S = 0.18$ and $dn_T/d\log k = -10^{-3}$ (dot line), $T/S = 0.0018$ and $dn_T/d\log k = 0$ (dash line) and $T/S = 0.0018$ and $dn_T/d\log k = -10^{-3}$ (dot-dash line) The sensitivity of space-, (correlated) ground-based detectors and the stochastic background from WD binaries is also shown for comparison.

is [36] $n_T = -(\bar{V}'/\bar{V})^2 M_{\text{Pl}}^2/(8\pi)$ and because of the slow-roll condition $|n_T| \ll 1$. Quite nicely, the spectral slope can be expressed in terms of the scalar contribution \mathcal{S} and tensorial contribution $\mathcal{T} \equiv 0.61\bar{V}/M_{\text{Pl}}$ to the quadrupole CMB anisotropy [see, e.g., Eqs. (3), (4) in Ref. [36]]. The result is $n_T = -\mathcal{T}/(7\mathcal{S})$.

The explicit expression of the GW spectrum is given by Eqs. (5), (6) in Ref. [36]. In Fig. 3 we plot the spectrum for two values of \mathcal{T}/\mathcal{S} , taking also into account the first-correction for the variation of the spectral slope with scale, $n_T(k)$, and compare it to the capabilities of LISA and (correlated^d) ground-based detectors. Figure 3 shows that if the predictions of standard inflation are correct, unfortunately there is no hope of observing the stochastic GW background from slow-roll inflation with current and planned GW detectors.

As seen from Fig. 3, in the case of LISA, primordial GW backgrounds

^dThe curves have been produced by multiplying LIGO I, LIGO II and LIGO III sensitivities curves shown in Fig. 1 by a constant factor obtained correlating Hanford (WA) and Louisiana (LO) LIGOs for four months at 90% confident level assuming a flat GW spectrum.

can be “covered” by the galactic WD binary background [37]. Even if two LISAs will be used, by correlating their data stream, the minimum achievable sensitivity is $\Omega_{\text{GW}} \geq 10^{-13}$ [37]. Thus, to probe $\Omega_{\text{GW}} \sim 10^{-16}$ – 10^{-15} from inflation with space-detectors of LISA-kind, the detectors have to operate outside the regime of mHz which is dominated by close WD binaries. Various scientists have already started discussing a follow-on mission of LISA. Given the current astrophysical understanding, the most promising region should be ~ 0.1 – 1 Hz [37, 38, 39, 40, 41], which can be obtained by shortening LISA arms by a factor of 100. In this higher frequency band the astrophysically generated background from unresolved NS binaries is present; however, because the number of sources per frequency bin is expected to be not very high, it should be possible to remove it. To achieve sensitivities on the order of $\Omega_{\text{GW}} \sim 10^{-16}$ – 10^{-15} , major, rather challenging improvements should be made, as increasing the laser power, the dimensions of the mirrors, etc..

The detection of relic GWs from inflation could be achieved also by measuring the polarization [42] in the CMBR with future CMB probes, as originally suggested in Ref. [43]. Indeed, the polarization tensor on the celestial sphere can be decomposed into its “gradient” and “curl” components. The scalar fluctuations do not have *handedness*, so they do not contribute to the curl, while tensorial fluctuations do contribute to the curl. If the polarization measurement will give a curl different from zero, GW will be detected and it will be possible to discriminate between the plethora of inflationary models currently available. Indeed, some of those models predict that the tensorial component \mathcal{T} is negligible.

In Sections 4.2, 4.3 we shall discuss other inflationary models. Before doing it, we want to point out that quite generally the tensorial perturbations will satisfy an equation similar to Eq. (28) but with the scale factor a replaced by the so-called “pump” field \tilde{a} . The pump field depends on the dynamics of the scale factor and the other fields which are part of the background. Following Refs. [44, 45, 54, 30], if we have two cosmological phases with $\tilde{a} = (\eta/\eta_*)^{\gamma_1}$ for $-\infty < \eta < \eta_1 < 0$ and $\tilde{a} = |(\eta - 2\eta_1)/\eta_1|^{\gamma_2}$ for $\eta_1 < \eta < \eta_2$, then the solutions of Eq. (28) (having replaced a with \tilde{a}) can be expressed in terms of Hankel functions of first and second species, as

$$\psi_k(\eta) = \sqrt{|\eta|} C H_{\nu_1}^{(1)}(k|\eta|), \quad (37)$$

$$\psi_k(\eta) = \sqrt{|\eta - 2\eta_1|} [\alpha_k H_{\nu_1}^{(1)}(k|\eta - 2\eta_1|) + \beta_k H_{\nu_1}^{(2)}(k|\eta - 2\eta_1|)], \quad (38)$$

where $\nu_1 = |\gamma_1 - 1/2|$ and $\nu_2 = |\gamma_2 - 1/2|$, and we have normalized Eq. (37) allowing only positive frequencies at $\eta \rightarrow -\infty$, so that $\psi_k \rightarrow C e^{-ik\eta}/\sqrt{k}$. It can be derived that the Bogoliubov coefficient β_k entering the GW spectrum is given by [30]

$$|\beta_f|^2 \sim f^{2\epsilon_T} \quad \begin{aligned} \epsilon_T &= 1 - |\gamma_1| - |\gamma_2| && \text{for } \gamma_1, \gamma_2 > 1/2 \quad \text{or} \quad \gamma_1, \gamma_2 < -1/2, \\ \epsilon_T &= -|\gamma_1 - \gamma_2| && \text{all other cases.} \end{aligned} \quad (39)$$

The spectral slope parameter n_T is defined by

$$n_T = \frac{d \log \Omega_{\text{GW}}}{d \log f} = 4 + 2\epsilon_T, \quad (40)$$

and it is directly related to the kinematic behaviour of the background, that is to the evolution of the curvature scale and Hubble parameter. If we apply the above equations to de Sitter inflation, we find that $\gamma_1 = -1$, for RD era $\gamma_2 = 1$ and for MD era $\gamma_2 = 2$. Thus, the spectral slope for fluctuations which re-enter the Hubble radius during RD era is $n_T = 0$, and for those which re-enter the Hubble radius during MD era is $n_T = -2$, in agreement with Eqs. (35), (36). Moreover, in the case of slow-roll or power-law inflation, $\gamma_1 < -1$, and it can be easily found that for fluctuations that re-enter the Hubble radius during RD era $n_T = 2 + 2\gamma_1 < 0$, as anticipated in Section 4.1.2.

Finally, we note that this way of estimating the spectral slope can be easily generalized [45] to the case of n cosmological phases occurring at times η_1, η_2, \dots if the pump fields follow a power-law evolution with coefficients $\gamma_1, \gamma_2, \dots$. In this case the relic GW spectrum is characterized by various frequency regions or *branches*, and in each of them the spectral slope depends *only* on the kinematics of the phases in which the mode associated to a given frequency went out of the Hubble radius and re-entered the Hubble radius. On the other hand, the amplitude of the GW spectrum and special features in it, like possible oscillations, are determined by the dynamics and by physical assumptions, such as when and how the reheating process took place, whether entropy production is produced at some later stages, etc..

4.2. Superstring-motivated cosmology

Potential-driven inflation of the kind discussed in Section 4.1 cannot be easily implemented in string theory if the dilaton field or a modulus field is simply identified with the inflaton field [46]. This result forced people to conceive new ways of reconciling inflation and string theory. Henceforth, we

shall briefly discuss some of those attempts which use supergravity description of superstring theory, the so-called pre-big-bang (PBB) scenario [47] and bouncing-Universe scenarios [48, 49]. Quite generally those scenarios predict a stochastic GW background anything but flat, which could be of interest for space- and ground-based detectors.

4.2.1. Pre-big-bang scenario

Due to the presence of other fields, at low energy superstring theory does not give Einstein general relativity – for example heterotic string theory in four dimensions is described by the action

$$\Gamma_{\text{eff}} = \frac{1}{2\lambda_s^2} \int d^4x \sqrt{|g|} e^{-\varphi} \left[\mathcal{R} + g^{\mu\nu} \partial_\mu \varphi \partial_\nu \varphi - \frac{1}{12} (dB)^2 - V(\varphi) \right], \quad (41)$$

where φ is the dilaton field, related to the string coupling by $g^2 = e^\varphi$; $dB = \partial_\mu B_{\nu\rho} + \partial_\nu B_{\rho\mu} + \partial_\rho B_{\mu\nu}$, where $B_{\mu\nu}$ is the two-form gauge field or antisymmetric field; $V(\phi)$ is a non-perturbative potential; and where λ_s is the string scale. In writing Eq. (41) we have disregarded for simplicity the internal dimensions, whose dynamics can be described in terms of moduli fields [47].

Henceforth, we limit the discussion to the homogeneous and isotropic case with $B = 0$ and $V = 0$ [$ds^2 = -dt^2 + a^2(t) d\vec{x}^2$, $\varphi = \varphi(t)$]. In this case the solution of the low-energy string-effective action (41) satisfies the scale-factor-duality symmetry: $a(t) \rightarrow 1/a(t)$, $\varphi(t) \rightarrow \varphi(t) - 6 \log a(t)$,^e with $a(t) \sim t^{1/\sqrt{3}}$ and $\varphi(t) \sim -\log t$. Noticing this property, Veneziano [50] conceived the idea of implementing the inflationary phase at times before the *would-be* big-bang singularity. Indeed, it is easily shown that for $t < 0$, $\dot{a} > 0$, $\ddot{a} > 0$, thus the Universe undergoes a (super) inflationary phase. Two different but physically equivalent descriptions of the PBB phase exist: either the string-frame picture described by Eq. (41), where the Universe undergoes an accelerated expansion ($H > 0$, $\dot{H} > 0$, $\dot{\varphi} > 0$), or the Einstein-frame picture, where the action (41) has the standard Hilbert-Einstein form and the evolution of the Universe is described by an accelerated contraction, or gravitational collapse ($H < 0$, $\dot{H} < 0$, $\dot{\varphi} > 0$).

This new kind of inflation, which can be shown solves the homogeneity and flatness conundra, is driven by the kinetic energy of the dilaton field and forces both the string coupling ($\dot{g} > 0$) and the spacetime curvature to grow toward the future. As a consequence, at least in the homogeneous

^eHere for convenience the origin of time has been fixed at $t = 0$.

case, the inflationary stage lasts for ever ($t \rightarrow -\infty$) and the initial state of the Universe is nearly flat, cold and decoupled: $g \ll 1$, $\mathcal{R}\lambda_s^2 \ll 1$.

The tensorial perturbations h_k in the PBB model satisfy an equation similar to Eq. (18) but with the scale factor a replaced by the pump field $\tilde{a} = e^{-\phi/2} a$, that is [44]

$$h_k''(\eta) + 2\frac{\tilde{a}'}{\tilde{a}} h_k'(\eta) + k^2 h_k(\eta) = 0. \quad (42)$$

Note that \tilde{a} coincides with the scale factor in the Einstein frame. [In the case of $D = d + n + 1$ dimensions with n internal dimensions contracting and d external dimensions expanding, isotropically, if tensorial perturbations depend only on the external dimensions, then Eq. (42) is still valid but the pump field $\tilde{a} = e^{-\phi/2} a^{(d-1)/2} b^{n/2}$, b being the scale factor of internal dimensions [44].] Let us consider the simplest scenario (henceforth minimal model) characterized by an isotropic superinflationary phase with static internal dimensions, followed by RD era. In this case, the solution of the background field equations is [47] $a(\eta) = (-\eta)^{(1-\sqrt{3})/2}$ and $\varphi(\eta) = \varphi_0 - \sqrt{3} \log(-\eta)$, and during RD era, $a(\eta) = (\eta - 2\eta_*)/(H_s \eta_*)$ and $\varphi(\eta) = \varphi_*$, where $H_s \simeq M_s = g_0 M_{\text{Pl}}$, with M_s the fundamental string mass and g_0 the string coupling at present time. Since during the superinflationary era the Hubble parameter is not constant ($\dot{H} \neq 0$), in fact it increases in time, we expect the GW spectrum for fluctuations re-entering the Hubble radius during RD era be non flat. Indeed, using Eq. (39) with $\gamma_1 = 1/2$ and $\gamma_2 = 1$, it can be easily derived that the spectral slope is [44, 52, 53] $n_T = 3$. If we assume that CMB photons we observe today carry the (red-shifted) energy of the primordial perturbations, i.e. $\Omega_\gamma(t_0) = (H_*/H_0)^2 (a_*/a_0)^4$, and at the end of the superinflationary phase $H_* \simeq H_s$ and $g_* \simeq g_0$, then the frequency at the end point of the spectrum is $f_* = k_*/(2\pi a_0) \simeq a_* H_s/(2\pi a_0) \sim 10^{10}$ Hz, and [44, 52, 53]

$$\Omega_{\text{GW}} = g_0^2 \Omega_\gamma(t_0) \left(\frac{f}{f_*} \right)^3. \quad (43)$$

Depending on the present value of the string coupling [51] $g_0 = 0.03\text{--}0.3$, the GW spectrum amplitude at the end point frequency is $\sim 10^{-7}\text{--}10^{-5}$ [$\Omega_\gamma(t_0) \sim 10^{-4}$], thus rather close to the BBN bound discussed in Section 3.4.1. In the right panel of Fig. 4 we show two examples of the stochastic GW background in the range of frequencies of space- and ground-based detectors. In the minimal model the spectrum has the peak in the GHz region and being elsewhere rather steep, it cannot be detected by current

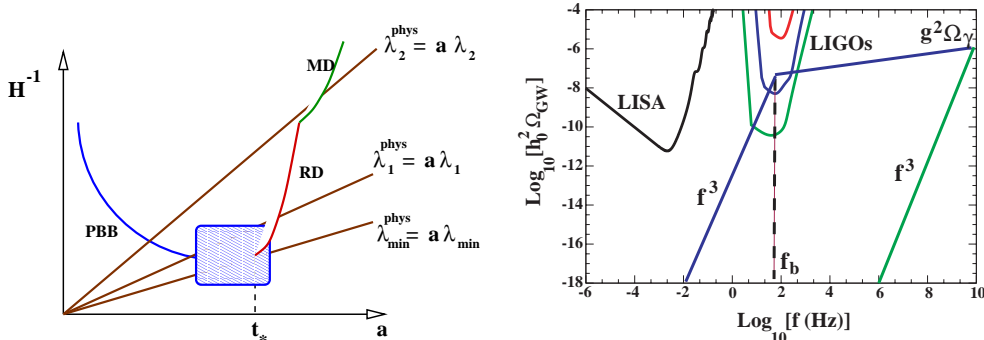


Figure 4. In the left panel we sketch the evolution of H and of some physical wavelengths during the superinflationary PBB phase, RD and MD eras. The shaded box refers to the spacetime region around the would-be big-bang singularity for which we do not have a complete description, yet. In the right panel we show two examples of the stochastic GW spectrum.

and planned GW detectors. Refs. [52, 53, 30] showed that if the PBB superinflationary phase is followed by other cosmological eras where (partial) higher-order derivatives and/or quantum loops corrections in the effective action (41) are included, the GW spectrum can have branches where it is less steeper, even flat, and could have amplitudes detectable by space- and ground-based detectors. However, robust predictions can be made only when a complete description of the transition from pre- to the post-big-bang era will be available, including the understanding of the big-bang singularity. Indeed, the spectral slope for $f > f_b$ in Fig. 4, depends crucially on the cosmological backgrounds around the would-be big-bang singularity.

4.2.2. Bouncing-Universe scenarios

New cosmologies motivated by string theory and influenced also by brane-world ideas have been proposed [48, 49]. As in the PBB model, in those scenarios it is assumed that the Universe had a long existence prior to the big bang singularity. Here, as an example, we shall focus on the bouncing-Universe model discussed in Ref. [49]. This model uses two four-dimensional boundary branes, one of which is the visible brane where our Universe lives, the other is the hidden brane. The two branes are originally separated by a finite distance which can be regarded, according to the M-theory conjecture [55], as the dilaton field in the strong-coupling regime. This scenario is

built on the following four-dimensional effective action on the visible brane (in Einstein frame):

$$\Gamma_{\text{eff}} = \frac{1}{16\pi G_{\text{N}}} \int d^4x \sqrt{|g|} \left[\mathcal{R} - \frac{1}{2} g^{\mu\nu} \partial_\mu \phi \partial_\nu \phi - V(\phi) \right]. \quad (44)$$

The hidden boundary brane (or bulk brane) is assumed to be initially in a state with minimal energy, and it is flat, parallel to the visible brane and at rest. Non-perturbative effects, for example due to a potential of the kind $V(\phi) = -V_0 e^{-c\phi}$ with $c > 0$, can generate interactions between the visible and bulk brane, causing the bulk brane to move toward the visible one and collide with it. In this way the kinetic energy of the bulk brane can be converted into radiation, and the hot big-bang era starts.

Differently from the PBB scenario, in the model of Ref. [49], the Universe evolves from strong ($g^2 = e^\phi \gg 1$) to weak coupling ($g^2 = e^\phi \ll 1$), and both in the string- and Einstein-frame it undergoes an accelerated contraction. Moreover, it is assumed that going toward the singularity ($\eta \rightarrow 0^-$) the potential V changes its shape and goes to zero. Thus the cosmological background in the Einstein frame can be roughly described by a phase with $a_{\text{E}}(\eta) \sim (-\eta)^\epsilon$ with $0 < \epsilon \ll 1$ (very slow contraction), followed by a phase with (almost) zero potential, i.e. a superinflationary phase of the PBB kind, with $a_{\text{E}}(\eta) \sim (-\eta)^{1/2}$ and then a RD era. The pump field \tilde{a} entering the equation of tensorial perturbations coincides with the scale factor in the Einstein frame ($\tilde{a} = a_{\text{E}}$), so for fluctuations which go out of the Hubble radius during the phase dominated by the potential and re-enter the Hubble radius during RD era, the discussion around Eqs. (38)–(39) gives: $\gamma_1 = \epsilon > 0$ and $\gamma_2 = 1$, thus $n_T \sim 2 + 2\epsilon$, whereas for fluctuations that go out of the Hubble radius during the phase with (almost) zero potential and re-enter during RD era, we recover the PBB result $n_T = 3$.

Hence, both the PBB and bouncing-Universe scenarios predict very steep GW spectra at very low frequency, so no contribution of tensorial fluctuations to the CMBR inhomogeneities. Thus, if a tensorial component will be found in CMBR, then the current version of those scenarios should be rejected.

Due to the collapse phase, in both scenarios discussed in this section the initial (classical) tensor fluctuations are not de-amplified [31], as occurs in potential-driven inflation (see discussion at the beginning of Section 4.1.1). This result, though paradoxical, does not imply that the initial value of tensor inhomogeneities must be fine tuned to unnaturally small value. In-

deed, it can be derived [31] that the energy density of tensor waves is indeed de-amplified. However, to solve the homogeneity problem in those superstring-inspired models, we have to apply constraints more severe [31] than in potential-driven inflation models.

It is worth to mention that some aspects of both the PBB and bouncing-Universe scenarios, have been questioned. Doubts on the naturalness of the initial conditions and on the actual solution of the homogeneity and flatness conundra were raised [56]. The formation of large-scale structures and CMBR inhomogeneities cannot be explained in those models as naturally as in the standard inflationary models (see Section 3.1) using adiabatic perturbations. [In the case of the PBB scenario, a way out has been recently suggested by converting isocurvature into adiabatic fluctuations [57] during the post-big-bang phase.] More importantly, a debate [58] on whether the scalar perturbations can be unambiguously calculated in those superstring-motivated models is still underway. Those issues can be clarified only when a complete and unique description of the transition from pre to post era will be available.

4.3. *Non-standard equations of state in post-big-bang eras*

In this section we want to give another example of non-flat relic GW spectrum due to the presence, soon after inflation, of a phase which differs from the RD era. The possibility of having an all variety of spectra by introducing non-standard, i.e. different from RD or MD, equations of state in post-big-bang eras was originally pointed out by Grishchuk [27].

An interesting example is the case in which the inflationary phase is followed by an expanding phase driven by an effective source whose equation of state is stiffer than radiation. Peebles and Vilenkin [59] discussed a model where the occurrence of a stiff post-inflationary phase is dynamically realized through a potential of the kind $V(\phi) = \lambda(\phi^4 + M^4)$ for $\phi < 0$ and $V(\phi) = \lambda M^8/(\phi^4 + M^4)$ for $\phi \geq 0$, with $\lambda \sim 10^{-14}$ and $M \sim 10^6$ GeV. This model has been denoted *quintessential inflation* and was originally introduced to explain the dark-energy conundrum, that is the present accelerated expansion of the Universe. The inflaton field starts its evolution at $\phi \ll -M_{\text{Pl}}$ and rolls toward zero. Inflation ends at $\phi \sim -M_{\text{Pl}}$ when significant part of the potential energy has turned into the kinetic energy of ϕ . The cosmological evolution is then driven by the kinetic energy of ϕ (the equation of state is $p = \rho$), thus the scale factor $a(\eta) \sim \sqrt{\eta}$. Following the discussion around Eqs. (38)–(39), we have $\gamma_2 = 1/2$, and

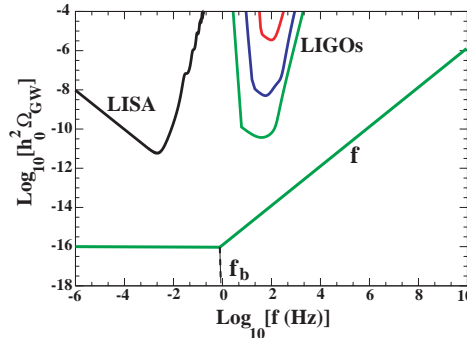


Figure 5. We show an example of the stochastic GW spectrum originated in quintessential inflation and contrast it with the sensitivity of space- and (correlated) ground-based GW detectors. For a detail discussion of the GW spectra as function of the free parameters see Ref. [60].

assuming that during quintessential inflation [60] $a(\eta) \sim -1/\eta$, we have $\gamma_1 = -1$. So, the spectral slope for fluctuations that exit the Hubble radius during quintessential inflation and re-enter the Hubble radius during the stiff era is $n_T = 1$ [59, 60]. The GW spectrum increases linearly as a function of the frequency. An example of such spectrum is shown in Fig. 5, where the flat branch refers to gravitons that go out of the Hubble radius during inflation and re-enter the Hubble radius during RD era. The peak of the spectrum is firmly localized at 100 GHz, with amplitude $\leq 10^{-6}$; the frequency f_b at which the flat branch starts depend on the free parameters in the model [60]. A very detailed analysis which includes the discussion of the free parameters entering the spectrum and the comparison with current and planned GW detectors can be found in Ref. [60]. Unfortunately, in Peebles and Vilenkin quintessential model [59] the spectrum is few orders of magnitudes below the sensitivity achievable with advanced ground-based detectors. As shown in Ref. [61], by relaxing the assumption the scalar field driving the kinetic-energy phase coincide with the inflaton field, it is possible to shift the spectrum ending frequency at lower frequencies and increase by few orders of magnitudes the amplitude of the GW spectrum in the frequency range of ground-based detectors.

5. Gravitational waves from cosmic strings

Topological defects could have been generated during symmetry-breaking phase transitions in the early Universe. Since the beginning of the 80s they received significant attention [62] as possible candidates for seeding structure formation. Recently, more accurate observations of CMBR inhomogeneities on smaller angular scales and compatibility with density-fluctuation spectrum on scales of $100 h_0^{-1}$ Mpc, restrict the contribution of topological defects to at most $\sim 10\%$ [63]. In the following, we shall restrict our discussion to cosmic strings formed when a $U(1)$ local gauge symmetry is spontaneously broken [see Ref. [64] for the possibility of producing cosmic strings from brane collision at the end of brane inflation scenario [65]].

Cosmic strings are characterized by a single dimensional scale: the mass-per-unit-length μ . Since they do not have any *ends*, they are in the form of loops, smaller or larger than the Hubble length. [The length of a string is defined as the energy of the loop divided by μ .] Those loops have very large mass-per-unit-length, on the order of $10^{22}g/cm$ if the scale at which the symmetry is broken is the GUT scale. Their tension is equal to their mass-per-unit-length, so they oscillate relativistically emitting GWs and shrinking in size. It is generally assumed, though difficult to prove, that a network of cosmic strings did form at some time during the evolution of the Universe. In this network the only relevant scale is the Hubble length. Small loops (smaller than Hubble radius length) oscillate, emit GWs and disappear, but they are all the time replaced by small loops broken off very long loops (longer than Hubble radius length). The wavelength of the GW is determined by the length of the loop, and since in the network there are loops of all sizes, the GW spectrum is (almost) flat in a large frequency band, extending from $f \sim 10^{-8}$ Hz to $f \sim 10^{10}$ Hz. The GW spectrum is nearly Gaussian and has been evaluated in detail in Refs. [66]. If r is the characteristic radius of the loop, the quadrupole moment is $Q \sim \mu r^3$ and by assuming an oscillation period of $\tau \sim r$, the energy emitted is $d\mathcal{E}/dt \sim P \sim G_N \ddot{Q}^2 \sim \gamma G_N \mu^2$, where γ is the dimensionless radiation efficiency ~ 60 . Numerical simulations of cosmic-string network would predict $\Omega_{\text{GW}} \sim P/\rho_c < 10^{-9}-10^{-8}$ for cosmic strings with $G_N \mu < 10^{-6}$. Thus, the Gaussian GW background from cosmic strings could be detectable by second and third generation of ground-based interferometers, and by LISA as well, being above the galactic stochastic GW background of WD binaries.

More recently, Damour and Vilenkin [67] found that strong beams of

high-frequency GWs could be produced at cusps (where the string reaches a speed very close to light velocity) and at kinks along the string loop. [In time domain they are “spikes” or “bursts”.] As a consequence of these beams the GW background discussed above becomes strongly non-Gaussian. The most interesting feature of these GW bursts is that they could be detectable for a large range of values of $G_N\mu$, larger than the usually considered search for the Gaussian spectrum. For example, if the average number of cusps in a string oscillation is only 10%, the GW bursts could be detectable by ground- and space-based detectors up to $G_N\mu \sim 10^{-13}$. If the number of cusps in a string oscillation is very small, kinks, which have smaller bursts but are ubiquitous, could generate a signal detectable by LISA for a large range of values of $G_N\mu$ [see Figs. 1, 2 in Ref. [67]].

The most stringent bound on the GW background from cosmic strings comes from pulsar timing [see Section 3.4.3]. The analysis of Ref. [67] suggests that the GUT value $G_N\mu_{\text{GUT}} \sim 10^{-6}$ is still compatible with existing pulsar data, and if accuracy will be improved, pulsar timing could allow to detect the GW bursts up to $G_N\mu \sim 10^{-11}$.

6. Gravitational waves from other mechanisms occurring in early Universe

During its history the Universe could have undergone phase transitions, corresponding to symmetry breaking of particle-physics fundamental interactions.

In a first-order phase transition the Universe is initially trapped in a high-temperature metastable phase (unbroken-symmetry phase), where the *false* vacuum is separated from the *true* vacuum by a barrier in the potential $V(\phi, T)$ of some scalar field ϕ driving the transition (ϕ is also called the order parameter) [see Fig 6]. The transition from the metastable to the ground state takes place via quantum tunneling across the barrier with random nucleation of bubbles: true vacuum is inside the bubbles, false vacuum is outside them. If the temperature when bubbles form is too high, they are born small, the volume energy cannot overcome the shrinking effect of the surface tension and they disappear quickly; but when the temperature drops below a critical temperature, bubbles are born larger, and since the latent heat released during the transition is converted to bubble-wall kinetic energy, they expand, approach velocity close to the speed of light, collide and leave the Universe in the broken-symmetry phase. When the collision occurs, the spherical symmetry is broken and GWs, as

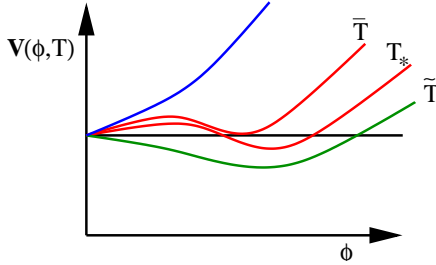


Figure 6. We show the typical temperature-dependence of a potential $V(\phi, T)$ in a first-order phase transition ϕ being the order parameter. At the temperature \bar{T} the true ($\langle \phi \rangle \neq 0$) and false (conventionally $\langle \phi \rangle = 0$) vacua are degenerate, and at \tilde{T} the false vacuum becomes unstable. The transition occurs at some temperature $\hat{T} < T_* < \bar{T}$

well as other particles [68], are radiated away [69]. Since the Universe is expanding, the temperature T_* at which the transition takes place can be obtained comparing the probability of bubble nucleation per unit time and volume with the expansion rate of the Universe at that temperature. The transition occurs when the probability for a single bubble to be nucleated within one horizon volume is on the order of one.

Two parameters determine the stochastic GW spectrum [70]: the bubble nucleation rate per unit volume β ($\Gamma = \Gamma_0 e^{\beta t}$) and the ratio α between the false vacuum energy density and the energy density of the radiation at the transition temperature T_* . The bubble collision produces a GW spectrum which is strongly peaked at the frequency characteristic of the nucleation rate, i.e. $2\pi f_{\text{peak}} \simeq \beta$. A detailed analysis gives [70]:

$$f_{\text{peak}} \simeq 5.2 \times 10^{-8} \left(\frac{\beta}{H_*} \right) \left(\frac{T_*}{1 \text{ GeV}} \right) \left(\frac{g_*}{100} \right)^{1/6} \text{ Hz}, \quad (45)$$

where H_* and g_* are the Hubble parameter and the number of degrees of freedom at the time of transition. Typical values for an electro-weak phase transition (EWPT) are $\beta/H_* \simeq 10^2\text{--}10^3$, $T_* = \mathcal{O}(100)$ GeV, for which $f_{\text{peak}} \simeq 10^{-4}\text{--}5 \times 10^{-3}$ Hz, and lies in the LISA frequency band. The GW spectrum was calculated in Ref. [70]; it reads

$$h_0^2 \Omega_{\text{GW}} \simeq 10^{-6} \kappa^2 \frac{\alpha^2}{(1+\alpha)^2} \frac{v_b^3}{0.24 + v_b^3} \left(\frac{H_*}{\beta} \right)^2 \left(\frac{100}{g_*} \right)^{1/3}, \quad (46)$$

where κ quantifies the fraction of latent heat that is transformed into bubble-wall kinetic energy and v_b is the bubble expansion velocity. At

frequencies lower than f_{peak} the GW spectrum $\propto f^{2.8}$ [70], while at higher frequencies it drops off as $\propto f^{-1.8}$ [70].

Non-perturbative calculations done using lattice field theory have shown that there is no first-order EWPT in the SM of particle physics for Higgs mass larger than W masses (current results predict an Higgs mass larger than W masses). In Minimal Supersymmetric Standard Models (MSSM), if the Higgs mass is in the range 110–115 GeV, there is the possibility of having a first-order phase transition, if the right-handed stop mass has a mass in the range 105–165 GeV [the stop particle is the scalar supersymmetric partner of the top quark]. However, in this case the GWs produced are too weak. For example, for a Higgs mass of 110 GeV and right-handed stop mass of 140 GeV, there exist regions in the parameter space where [71] $\alpha \sim 10^{-2}$, $\kappa \sim 0.05$ and $H_*/\beta \simeq 10^{-4}$ and thus $h_0^2 \Omega_{\text{GW}} \sim 10^{-19}$ around 10 mHz. The strength of the transition can be enhanced in next-to-minimal supersymmetric standard models (NMSSM). Apreda et al. [71] investigated the NMSSM obtained adding a gauge singlet in the Higgs sector [72]. This model is rather attractive also because it can explain the observed baryon asymmetry. Apreda et al. found that there exist regions in the parameter space for which the GW spectrum is $h_0^2 \Omega_{\text{GW}} \sim 10^{-15}$ – 10^{-10} at $f_{\text{peak}} \simeq 10$ mHz. Note that for frequencies 10^{-4} – 3×10^{-3} Hz the stochastic GW background from WD binaries could “cover” the GW spectrum from first-order phase transitions. If this GW background will be ever detected it will be a signature of supersymmetry and, combined with experimental bounds from future particle colliders, it could allow to discriminate between various supersymmetric models.

A stochastic GW background could be also produced during a first-order phase transition from turbulent (anisotropic) eddies generated in the background fluid during the fast expansion and collision of the true-vacuum bubbles [70, 71, 73]. In the NMSSM [72] there exist regions of the parameter space where [71] $h_0^2 \Omega_{\text{GW}} \sim 10^{-10}$ with peak frequency in the mHz. Recently, the authors of Ref. [74] evaluated the stochastic GW background generated by cosmic turbulence before neutrino decoupling, i.e. much later than EWPT, and at the end of a first-order phase transition if magnetic fields also affect the turbulent energy spectrum. The observational perspectives of those scenarios are promising for LISA.

Turner and Wilczek [75] pointed out that if inflation ends with bubble collisions, as in extended inflation, the GW spectrum produced has a peak in the frequency range of ground-based detectors. Subsequent analyses have shown that in two-field inflationary models where a field performs

the first-order phase transition and a second field provides the inflationary slow rolling (so-called first-order or false vacuum inflation [76]), if the phase transition occurs well before the end of inflation, a GW spectrum peaked around $10\text{--}10^3$ Hz, can be produced [77], with an amplitude large enough, depending on the number of e-foldings left after the phase transition, to be detectable by ground-based interferometers. A successful detection of such a spectrum will allow to distinguish between inflation and other cosmological phase transitions, like QCD or electroweak, which have a different peak frequency.

Another mechanism that could have produced GWs in the early universe is parametric amplification after preheating [78]. During this phase classical fluctuations produced by the oscillations of the inflaton field ϕ can interact back, via parametric resonance, on the oscillating background producing GWs. In the model where the inflaton potential contains also the interaction term $\sim \phi^2 \chi^2$, χ being a scalar field, the authors of Ref. [78] estimated $\Omega_{\text{GW}} \sim 10^{-12}$ at $f_{\text{min}} \sim 10^5$ Hz, while in pure chaotic inflation $\Omega_{\text{GW}} \leq 10^{-11}$ at $f_{\text{min}} \sim 10^4$ Hz. [See Fig. 3 in Ref. [78] for the GW spectrum in the range $10^6\text{--}10^8$ Hz.] Unfortunately, the predictions lie in frequency range where no GW detectors have been planned so far, although EM cavities to detect GWs were proposed [79].

7. Gravitational waves in brane world scenarios

During the last years there have been feverish activities around brane-world models [80, 81]. Those scenarios are based on the idea that large ($\geq 1/M_{\text{Pl}}$) spatial, extra dimensions might exist. They assume that ordinary matter is confined onto a three-dimensional subspace, called the (visible) *brane*, which is embedded in a larger space, called the *bulk*. Only gravitational interactions are allowed to propagate in the bulk. If n is the number of extra dimensions, then the four-dimensional Planck mass M_{Pl} is a derived quantity, while the fundamental scale is determined by the gravitational mass M_{fund} in $n + 4$ dimensions. In the case of a flat bulk, l being the typical length of the extra dimensions, $M_{\text{Pl}}^2 = M_{\text{fund}}^{n+2} l^n$ with M_{fund} ranging between TeV to M_{Pl} . In the following, we shall mention results obtained in five-dimensional brane-world models ($n = 1$).

By normalizing properly Eq. (32) and taking the limit $k\eta \ll 1$, it is easily derived that long-wavelength GWs generated in de Sitter inflation have a (almost) constant amplitude $k^{3/2} h_k = H_{\text{dS}}/M_{\text{Pl}}$, which depends on the two scales in the problem: the Hubble parameter during inflation

and the low-energy Planck mass. In five-dimensional brane-world models there is an additional scale in the problem, the scale l associated to the fifth dimension. Quite generically, we could expect [82] that if inflation on the (visible) brane occurs at scales smaller than the curvature of the extra dimension, i.e. $Hl \gg 1$, then the amplitude of GWs ^f can be modified with respect to the value predicted in standard four-dimensional theory – for example [83, 84, 85, 82] $k^{3/2} h_k = f(Hl) H/M_{\text{Pl}}$ with some function f . ^g In the brane-world models analysed in Refs. [83, 84, 82], it was found that for $Hl \gg 1$ the tensor amplitude is enhanced with respect to the standard result, i.e. $f(Hl) > 1$. Moreover, the ratio between scalar and tensorial perturbations \mathcal{T}/\mathcal{S} may also differ from the value predicted by standard four-dimensional theory [83, 82] and it could depend on specific features of the brane-inflation model. However, as seen in Section 3, the overall shape of the relic GW spectrum depends not only on the evolution of the tensor-mode amplitude during inflation but also on the post-big-bang phases, i.e. on the era at which the mode re-enters the Hubble radius. Only when those cosmological phases will be consistently described in the brane-world scenarios, we will have robust predictions for the GW spectrum.

By implementing quintessential inflation on the visible brane, and evaluating the Bogoliubov coefficients all along the Universe evolution, the authors of Ref. [86] found results similar to the ones discussed in Section 4.3: the GW spectrum has a branch where it increases linearly as function of the frequency.

GWs can be also produced by excitations of the so-called radion field, which controls the size of the extra dimension, and by inhomogeneities in the displacement of the brane [87]. Those waves should peak at a frequency fixed by the scale of the extra dimension. LISA could observe excitations emitted at scales from millimeters to microns, while ground-based interferometers could observe rather small extra dimensions, up to $\sim 10^{-12}$ mm.

In some brane world scenarios the causal propagation of gravitational and luminous signals can be different [88, 89]. In the case of an asymmetric warped spacetime of the kind [89],

$$ds^2 = -n^2(l) dt^2 + a^2(l) \left(\frac{dr^2}{1 - k r^2} + r^2 d\Omega_2^2 \right) + b^2(l) dl^2, \quad (47)$$

^fHere the GW refers to the homogeneous Kaluza-Klein massless mode. Massive Kaluza-Klein gravitons decay very fastly [83, 84, 82], so their production is very suppressed during brane inflation.

^gIn the models analysed by Frolov and Kofman [82], $f(Hl)/M_{\text{Pl}} = 1/M_{\text{Pl,inf}}$ where $M_{\text{Pl,inf}}$ is the Planck mass during inflation.

where l is the coordinate along the extra dimension, and $k = \pm 1, 0$ is the spatial curvature of the three-dimensional sections parallel to the brane, the local speed of light $c(l) = n(l)/a(l)$ depends on the position l along the extra dimension. Since GWs can propagate in the bulk, a GW signal emitted at point \mathcal{A} on the brane can take [if $c(l)$ is increasing away from the brane] a *short-cut* in the bulk, and to an observer located at point \mathcal{B} on the brane it appears quicker than a photon traveling along the brane from \mathcal{A} to \mathcal{B} . If true, this effect predicts a difference between gravitational and luminous speed. By detecting GWs and EM waves from γ -ray bursts and supernovae, ground-based detectors of second generation can put upper limits on $\delta c/c$ at most on the order of 10^{-17} [12] for γ -ray bursts, and 10^{-11} for a supernova in the Virgo cluster of galaxies.

8. Extraction of cosmological parameters from detection of GWs

In this section we want to discuss very briefly another possible way GW detection can be used to probe cosmology, although not directly the physical mechanisms occurring in the very early Universe.

It was realized long ago that binaries made of compact bodies, like BHs or NSs, which spiral in toward each other losing energy because of the emission of GWs, are “standard candles” [90]. Indeed, once the binary masses and spins, position and orientation angles are specified, the GW signal passing-by the detector depends only on the luminosity distance $d_L(z, \Omega_M, \Omega_\Lambda, \dots)$ between binary and detector. By using three ground-based interferometers or LISA (and suitably high signal-to-noise ratio) it is possible to determine the location and orientation of the binary in the sky, extract the masses, the spins and the cosmological distance but not the source’s cosmological red-shift. Indeed, the inspiral GW signal emitted from a binary with masses (m_1, m_2) at red-shift z cannot be distinguished, except for an overall factor in the amplitude, from the one emitted from a local binary with masses $[(1+z)m_1, (1+z)m_2]$. To break the degeneracy and obtain the distance–red-shift curve and the cosmological parameters, one could associate the binary-coalescence event to an EM event which had very clear emission or absorption lines, from which one could read z . [Because the errors in position determinations can be rather large, the existence of EM counterpart can also improve the accuracy in measuring the luminosity distance – for example by mapping massive BH binaries with LISA $\delta d_L/d_L$ decreases from 1–10% to 0.15–1% [91].] However, Holz and

Hughes [91] recently pointed out that, practically, because of gravitational-lensing effects (GWs are lensed as EM radiation are lensed) the precision with which the luminosity distance can be determined is degraded, though still slightly better than what Type-Ia supernovae probes can reach, but unless the event rates is high enough the extraction of cosmological parameters cannot be done with good accuracy.

9. Summary

As seen, the search for GWs from the very early Universe is rather challenging but the outcome is certainly worth the effort.

Theoretically, so little we know about the very early evolution of our Universe, that the predictions for the stochastic GW background from standard inflation [27, 28] and/or superstring-motivated models [47, 48], including also brane-world scenarios [83, 84, 85, 86, 87], should be considered just as indications. What we learned from those models, is that it could well be the GW spectrum is not (almost) flat all the way from $f \sim 10^{-16}$ Hz to $f \sim 10^{10}$ Hz. There could be frequency regions in which it increases or decreases [27] due to cosmological phases existed before the would-be big-bang singularity, and/or post-big-bang phases with equations of state different than radiation or matter ones, whose presence we cannot currently exclude. [Even an initial state different from vacuum could affect the relic GW spectrum [34], as seen from Eq. (27).] Future CMB polarization experiments [43] could detect the tensor contribution at very large wavelength and discriminate within plethora of inflationary models. The detection of GWs from bubble collision [69, 71, 76, 77] and/or turbulent motion [69, 71, 73, 74] in the primordial plasma, and especially the frequency at which the GW spectrum is peaked, will reveal if first-order phase transitions occurred, and at which particle physics mechanism they are associated to: QCD, EW, last stages of inflation, etc. If a network of cosmic strings ever formed, it should have produced a Gaussian [66] or even strongly non-Gaussian [67] GW spectrum, which could be detectable by the second generation of ground-based interferometers and LISA. If not observed, we could put upper limits on few free parameters. An independent estimation of the cosmological parameters could be obtained by detecting GWs from coalescing binaries at fairly high red-shift [90, 91].

Experimentally, since the GW signal from astrophysical sources is much more promising than the one from the early Universe, the ground- and space-based detectors were conceived and designed to detect the formers.

Various scientists in the GW community have already started thinking at future detectors, like the follow-on LISA missions which could focus more on early-time cosmological signals [37, 38, 39, 40, 41]. The technological challenges for these missions are considerable and deserve very careful investigations. Finally, ground-based GW detectors in the high-frequency region of MHz [79] and GHz [22] have gained more attention [47, 60, 78].

So, even if the detection of GWs from primordial Universe is still somewhat far ahead of us, maybe, if nature is kind with us, we will not wait for a long time. There could be surprises.

Acknowledgments

I wish to thank the organizers of the TASI school for having invited me to such a pleasant and stimulating school and all the students for their interesting questions. In preparing and writing these lectures I benefited from conversations with Yanbei Chen, Scott Hughes, Marc Kamionkowski, Arthur Kosowsky, David Langlois, Shane Larson, Albert Lazzarini, Michele Maggiore, Jérôme Martin, Alberto Nicolis, Sterl Phinney, Patricia Purdue and Kip Thorne.

This research was also supported by Caltech's Richard Chace Tolman Foundation.

References

- [1] A. Einstein, *Sitzber. Preuss. Akad. Wiss.*, 688 (1916); see also *Preuss. Akad. Wiss.*, 154 (1918).
- [2] H. Bondi, *Nature* **179**, 1072 (1957); *ibid.* **186**, 535 (1960).
- [3] R. Hulse and J. Taylor, *Astrophys. J.*, **324** (1975).
- [4] P. Astone et al., *Europhys. Lett.* **12**, 5 (1990); G. Pallottino, in "Gravitational Waves, Sources and Detectors," p 159 (Singapore, World Scientific, 1997); E. Mauceli et al., *Phys. Rev.* **D54**, 1264 (1996); D. Blair et al., *Phys. Rev. Lett.* **74**, 1908 (1995); M. Cerdonio et al., *Class. Quantum Grav.* **14**, 1491 (1997).
- [5] M. Ando et al., *Phys. Rev. Lett.* **86**, 3950 (2001); A. Abramovici et al., *Science* **256**, 325 (1992); H. Lück et al., *Class. Quantum Grav.* **14**, 1471 (1997); B. Caron et al., *Class. Quantum Grav.* **14**, 1461 (1997).
- [6] See, e.g, Sections III and IV in S.A. Hughes, S. Marka, P.L. Bender and C.J. Hogan, [astro-ph/0110349].
- [7] B.J. Meers and K. Strain, *Phys. Rev.* **A44**, 4693 (1991); J. Mizuno et al., *Phys. Lett.* **A175**, 273 (1993); E. Gustafson, D. Shoemaker, K.A. Strain and R. Weiss, "LSC White paper on detector research and development," www.ligo.caltech.edu/docs/T/T990080-00.pdf.
- [8] A. Buonanno and Y. Chen, *Phys. Rev. D* **64**, 042006 (2001).

- [9] V.B. Braginsky and F.Ya. Khalili, *Phys. Lett.* **A147**, 251 (1990); V.B. Braginsky, M.L. Gorodetsky, F.Ya. Khalili and K.S. Thorne, *Phys. Rev.* **A61**, 044002 (2000).
- [10] P. Purdue, *Phys. Rev.* **D66**, 022001 (2001); P. Purdue and Y. Chen, *Phys. Rev.* **D66**, 122004 (2002).
- [11] References on LISA project can be found at <http://www.lisa.uni-hannover.de/lisapub.html>.
- [12] C. Cutler and K.S. Thorne, [gr-qc/0204090].
- [13] B. Allen, *Lectures at Les Houches School*, 1996 [gr-qc/9604033].
- [14] M. Maggiore, *Phys. Rep.* **331**, 283 (2000).
- [15] K.S. Thorne, *Gravitational radiation*, in *300 Years of Gravitation* ed. by S.W. Hawking and W. Israel (Cambridge University Press, Cambridge, 1987).
- [16] N. Christensen, *Phys. Rev.* **D46**, 5250 (1992); E.E. Flanagan, *Phys. Rev.* **D48**, 2389 (1993); B. Allen and J.D. Romano, *Phys. Rev.* **D59**, 102001 (1999).
- [17] N. Cornish, *Phys. Rev.* **D65**, 022004 (2000); N. Cornish and S. Larson, *Class. Quantum Grav.* **18**, 3473 (2001).
- [18] J.W. Armstrong, F.B. Estabrook and M. Tinto, *Class. Quantum* **18**, 4059 (2001); M. Tinto, J.W. Armstrong and F.B. Estabrook, *Phys. Rev.* **D63**, 021101(R) (2001).
- [19] C. Ungarelli and A. Vecchio, *Phys. Rev.* **D64**, 121501 (2001).
- [20] Ya.I. Zel'dovich and I.D. Novikov, "The structure and evolution of the Universe," (Chicago, University of Chicago Press, 1983), p 157.
- [21] E.W. Kolb and M.S. Turner, "The early Universe," (Addison Wesley, Reading Massachusetts, 1990).
- [22] E. Iacopini, E. Picasso, F. Pegoraro, and L.A. Radicati, *Phys. Lett* **73A**, 140 (1979); C.M. Caves, *Phys. Lett.* **80B**, 323 (1979).
- [23] See, e.g., Lectures by K.A. Olive in this Proceedings.
- [24] C.J. Copi, D.N. Schramm and M.S. Turner, *Phys. Rev.* **D55**, 3389 (1997).
- [25] B. Allen and S. Koranda, *Phys. Rev.* **D50**, 3713 (1994).
- [26] S. Thorsett and R. Dewey, *Phys. Rev.* **D53**, 3468 (1996).
- [27] L. Grishchuk, *Sov. Phys. JETP* **40**, 409 (1974); *Class. Quantum Grav.* **10**, 2449 (1993).
- [28] A. Starobinsky, *JETP Lett.* **30**, 682 (1979).
- [29] N.D. Birrell and P.C.W. Davis, "Quantum fields in curved space," (Cambridge, Cambridge University Press, 1982).
- [30] A. Buonanno, K. Meissner, C. Ungarelli and G. Veneziano, *JHEP* **001**, 004 (1998).
- [31] A. Buonanno and T. Damour, *Phys. Rev.* **D50**, 3713 (2001).
- [32] See, e.g., Lectures by S. Carroll in this Proceedings.
- [33] L.F. Abbott and D.D. Harari, *Nucl. Phys.* **B264**, 487 (1986); B. Allen, *Phys. Rev.* **D37**, 2078 (1988).
- [34] L. Hui and W.H. Kinney, *Phys. Rev.* **D65**, 103507 (2002).
- [35] L. Krauss and M. White, *Phys. Rev. Lett.* **69**, 869 (1992).
- [36] M. S. Turner, *Phys. Rev.* **D55**, R435 (1996).
- [37] C. Ungarelli and A. Vecchio, *Phys. Rev.* **D63**, 064030 (2001).
- [38] N. Seto, T. Kawamura and T. Nakamura, *Phys. Rev. Lett.* **87**, 221103 (2001).

- [39] C.J. Hogan and P.L. Bender, *Phys. Rev.* **D64**, 062002 (2001).
- [40] S. Phinney, (private communication).
- [41] K.S. Thorne, (private communication).
- [42] See, e.g., Lectures by M. Zaldarriaga in this Proceedings.
- [43] M. Kamionkowski, A. Kosowsky and A. Stebbins, *Phys. Rev.* **D55**, 7368 (1997); U. Seljak and M. Zaldarriaga, *Phys. Rev.* **D78**, 2054 (1997); M. Kamionkowski and A. Kosowsky, *Phys. Rev.* **D57**, 685 (1998).
- [44] M. Gasperini and M. Giovannini, *Phys. Rev.* **D47**, 1519 (1993).
- [45] M. Gasperini, [hep-th/9604084].
- [46] B.A. Campbell, A.D. Linde and K.A. Olive, *Nucl. Phys.* **B335**, 146 (1991); R. Brustein and P.J. Steinhardt, *Phys. Lett.* **B302**, 196 (1993).
- [47] G. Veneziano and M. Gasperini, [hep-th/0207130].
- [48] J. Khoury, B.A. Ovrut, P.J. Steinhardt and N. Turok, *Phys. Rev.* **D64**, 123522 (2001).
- [49] J. Khoury, B.A. Ovrut, N. Seiberg, P.J. Steinhardt and N. Turok, *Phys. Rev.* **D65**, 086007 (2002).
- [50] G. Veneziano, *Phys. Lett.* **B265**, 287 (1991).
- [51] V. Kaplunovsky, *Phys. Rev. Lett.* **55**, 1036 (1985).
- [52] R. Brustein, G. Gasperini, G. Giovannini and G. Veneziano, *Phys. Lett.* **B361**, 45 (1995).
- [53] A. Buonanno, M. Maggiore and C. Ungarelli, *Phys. Rev.* **D55**, 3330 (1997).
- [54] M. Gasperini, *Phys. Rev.* **D56**, 4815 (1997); [hep-th/9907067].
- [55] P. Hôrava and E. Witten, *Nucl. Phys.* **B460**, 506 (1996).
- [56] M.S. Turner and E.J. Weinberg, *Phys. Rev.* **D56**, 4604 (1997); N. Kaloper, A. Linde and R. Bouso, *Phys. Rev.* **D59**, 043508 (2001); A. Linde, [hep-th/0205259].
- [57] V. Bozza, M. Gasperini, M. Giovannini and G. Veneziano, *Phys. Lett.* **B543**, 14 (2002); [hep-ph/0212112].
- [58] R. Brustein, M. Gasperini, M. Giovannini, V. Mukhanov and G. Veneziano, *Phys. Rev.* **D51**, 6744 (1995); D.H. Lyth, *Phys. Lett.* **B526**, 173 (2002); R. Brandenberger and F. Finelli, *JHEP* **0111**, 056 (2001); J. Martin, P. Peter, N. Pinto-Neto and D.J. Schwarz, *Phys. Rev.* **D65**, 123513 (2002); R. Durrer and F. Vernizzi, *Phys. Rev.* **D66**, 083503 (2002).
- [59] P.J.E. Peebles and A. Vilenkin, *Phys. Rev.* **D59**, 063505 (1999).
- [60] M. Giovannini, *Phys. Rev.* **D60**, 123511 (1999).
- [61] A. Riazuelo and J.P. Uzan, *Phys. Rev.* **D62**, 083506 (2000).
- [62] A. Vilenkin, *Phys. Rep.* **121**, 263 (1985).
- [63] F.R. Bouchet, P. Peter, A. Riazuelo and M. Sakellariadou, *Phys. Rev.* **D65**, 021301 (2001).
- [64] S. Sarangi and S.H. Tye, *Phys. Lett.* **B536**, 185 (2002).
- [65] G. Dvali and S.H. Tye, *Phys. Lett.* **B450**, 72 (1999).
- [66] R.R. Caldwell and B. Allen, *Phys. Rev.* **D45**, 3447 (1992); R.R. Caldwell, R.A. Battye and E.P.S. Shellard, *Phys. Rev.* **D54**, 7146 (1996).
- [67] T. Damour and A. Vilenkin, *Phys. Rev. Lett.* **85**, 3761 (2000); *Phys. Rev.* **D64**, 064008 (2001).
- [68] C.J. Hogan, *Phys. Lett.* **B133**, 172 (1983); E. Witten, *Phys. Rev.* **D30**, 272

- (1984); C.J. Hogan, *Mon. Not. R. Astr. Soc.* **218**, 629 (1986).
- [69] A. Kosowsky, M.S. Turner and R. Watkins, *Phys. Rev.* **D45**, 4514 (1992); *Phys. Rev. Lett.* **69**, 2026 (1992); A. Kosowsky and M.S. Turner, *Phys. Rev.* **D47**, 4372 (1993); M. Kamionkowski, A. Kosowsky and M.S. Turner, *Phys. Rev.* **D49**, 2837 (1994).
- [70] see M. Kamionkowski, A. Kosowsky and M.S. Turner in Ref. [69].
- [71] R. Apreda, M. Maggiore, A. Nicolis and A. Riotto, *Class. Quant. Grav.* **18**, L155-L162 (2001); *Nucl. Phys.* **B631**, 342 (2002); A. Nicolis, PhD Thesis 2002, Scuola Normale Superiore, Pisa, Italy.
- [72] J. Ellis, J.F. Gunion, H.E. Haber, L. Roszkowski and F. Zwirner, *Phys. Rev.* **D39**, 844 (1989).
- [73] A. Kosowsky, A. Mack and T. Kahniashvili, *Phys. Rev.* **D66**, 024030 (2002).
- [74] A.D. Dolgov and D. Grasso, *Phys. Rev. Lett.* **88**, 011301 (2002); A.D. Dolgov, D. Grasso and A. Nicolis, *Phys. Rev.* **D66**, 103505 (2002).
- [75] M.S. Turner and F. Wilczek, *Phys. Rev. Lett.* **65**, 3080 (1990).
- [76] See, e.g., M.S. Turner, E.J. Weinberg and L.M. Widrow, *Phys. Rev.* **D46**, 2384 (1992); E.J. Copeland, A.R. Liddle, D.H. Lyth, E.D. Stewart and D. Wands, *Phys. Rev.* **D49**, 6410 (1994).
- [77] C. Baccigalupi, L. Amendola, P. Fortini and F. Occhionero, *Phys. Rev.* **D56**, 4610 (1997).
- [78] S. Khlebnikov and I. Tkachev, *Phys. Rev.* **D56**, 653 (1997).
- [79] V.B. Braginski, L.P. Grishchuck, A.G. Doroshkevich, Ya.B. Zeldovich, I.D. Novikov and M.V. Sazhin, *Sov. Phys. JETP* **38**, 865 (1974).
- [80] N. Arkani-Hamed, S. Dimopoulos and G.R. Dvali, *Phys. Lett.* **B429**, 263 (1998); I. Antoniadis, N. Arkani-Hamed, S. Dimopoulos and G.R. Dvali, *Phys. Lett.* **B436**, 257 (1998); L. Randall and R. Sundrum, *Phys. Rev. Lett.* **83**, 3370 (1999); *ibid.* **83**, 4690 (1999).
- [81] See, e.g., Lectures by C. Csáki in this Proceedings.
- [82] A. Frolov and L. Kofman, [hep-th/0209133].
- [83] D. Langlois, R. Maartens and D. Wands, *Phys. Lett.* **B489**, 259 (2000).
- [84] D. Gorbunov, V.A. Rubakov and S.M. Sibiryakov, *JHEP* **10**, 015 (2001).
- [85] G.F. Giudice, E.W. Kolb, J. Lesgourgues and A. Riotto, *Phys. Rev.* **D66**, 083512 (2002).
- [86] V. Sahni, M. Sami and T. Souradeep, *Phys. Rev.* **D65**, 023518 (2001).
- [87] C.J. Hogan, *Phys. Rev. Lett.* **85**, 2044 (2000); *Phys. Rev.* **D62**, 121302(R) (2000).
- [88] D. Chung and K. Freese, *Phys. Rev.* **D62**, 063513 (2000); H. Ishihara, *Phys. Rev. Lett.* **86**, 381 (2001); R. Caldwell and D. Langlois, *Phys. Lett.* **B511**, 129 (2001).
- [89] C. Csáki, J. Erlich and C. Grojean, *Gen. Rel. Grav.* **33**, 1921 (2001); *Nucl. Phys.* **B604**, 312 (2001).
- [90] B.F. Schutz, *Nature* **323**, 310 (1985); B.F. Schutz and Krolak, *Gen. Relativ. Grav.* **19**, 1163 (1987); D. Marković, *Phys. Rev.* **D48**, 4738 (1993); D.F. Chernoff and L.S. Finn, *Astrophysical Journal* **411**, L5 (1993).
- [91] D. Holz and S.A. Hughes, [astro-ph/0212218].